Hydrogen Bonding between Acetone and Silica Gel, as Studied by NMR

Vicky H. Pan, Ting Tao, Jian-Wei Zhou, and Gary E. Maciel*

Department of Chemistry, Colorado State University, Fort Collins, Colorado 80523

Received: March 22, 1999; In Final Form: May 5, 1999

^{13}C NMR spectra and relaxation parameters (T_1^H, T_1^C, $T_{1\rho}^H$, T_{CH}) were measured via CP-MAS and DP-MAS techniques as a function of acetone loading level in acetone/SiO_2 samples at 25 °C. T_1^H and $T_{1\rho}^H$ values were also measured via ^{29}Si CP-MAS experiments. Peak positions and relaxation parameters are averaged by rapid exchange between different acetone interaction sites on the surface. The data were analyzed in terms of a surface equilibrium of adsorbed acetone units between hydrogen-bonding and non-hydrogen-bonding sites. Data analysis by this model yielded the surface concentration of hydrogen-bonding (silanol) sites (1.5 nm^{-2}) and the equilibrium constant ($K = 3.0$ nm^2). Variable-temperature experiments (124−297 K) at three loading levels yielded values of $\Delta H°$ (-5.8 ± 0.3 kJ mol^{-1}) and $\Delta S°$ (-12.5 ± 0.7 J K^{-1} mol^{-1}). A self-consistent, qualitative interpretation of measured relaxation parameters is made in terms of the relative mobilities of hydrogen-bonded (less mobile) and non-hydrogen-bonded (more mobile) acetone on the SiO_2 surface.

Introduction

Silica surfaces play important roles in numerous areas in both pure and applied sciences.[1−3] These areas include such diverse topics as fundamental surface chemistry, surface derivatization, chromatography, composite interfaces, and supported catalysts. Many of the technologically important properties of the silica surface depend on its surface-bound OH groups, based on SiOH (silanol) moieties. Silanols are well-known for their Brönsted acid and hydrogen-bonding characteristics and for their participation in the formation of linkages to a variety of tethered groups, e.g., via silylation.[4−6]

Acetone is not only an important industrial solvent but also, as the simplest member of the ketone family, it represents this important structural type in a variety of chemical reactions and interactions based on its carbonyl group. In view of the capability of the oxygen site of a ketone's carbonyl group to function as a basic site, it is not surprising that hydrogen bonding between acetone and suitable hydrogen-bonding acids is well established.[7,8] Hence, the acetone/silica system is a reasonable choice for studying the adsorption of acetone on surfaces containing bound OH groups, with the expectation that the properties of this system will be dominated, at least for a range of compositions, by hydrogen-bonded complexes. Indeed, there are prior published studies, based on a variety of techniques, focusing on the acetone/silica system.[9−25]

Infrared (IR) spectroscopy has been used to study the acetone/SiO_2 system and confirmed the existence of the $(CH_3)_2CO\cdots H-O\langle Si\rangle$ complex (where $\langle Si\rangle$ represents a silicon atom at the silica surface).[9−13] Prior ^{13}C NMR studies of the acetone/SiO_2 system have also been reported,[22−25] but these have not been based on the usual line-narrowing techniques employed in modern NMR ^{13}C experiments on solids or solid surfaces, e.g., magic-angle spinning (MAS) and high-power (dipolar) ^{1}H decoupling.[26−29]

These prior NMR studies have shown, as expected from earlier ^{13}C NMR studies of a variety of ROH/acetone solutions,[7,8] the existence of hydrogen-bonded complexes. Bernstein and co-workers interpreted their ambient-temperature ^{13}C NMR and infrared data in terms of a model based on an equilibrium between "free molecules" of acetone (presumably in the gaseous state) and silica adsorption sites that apparently include geminal OH groups, "isolated (free) OH groups", nonhydroxylic adsorption sites, and surface complexes.[25] While the model we employ in our data analysis (vide infra) differs substantially from this model, the algebraic expressions developed by Bernstein et al. are also applicable to our analysis. One of the models considered by Borovkov and co-workers[24] in the analysis of their ambient-temperature ^{13}C NMR data is the same model as we employ below, i.e., a rapid equilibrium of adsorbed acetone between hydrogen-bonding and non-hydrogen-bonding sites on the silica surface. Both Gay and co-workers[22] and Slotfeldt-Ellingsen and co-workers[23] studied the acetone/silica system over a range of temperatures but did not employ models conducive to extracting thermodynamic parameters of interest; the latter group attempted to distinguish between adsorption in different monolayers in interpreting their data. These earlier ^{13}C NMR studies did not include consideration of relaxation data and side-stepped the general issue of whether major intensity components were missed because solid-state line-narrowing techniques were not used.

In the study reported here, ^{13}C NMR spectra were obtained on acetone/SiO_2 samples, based largely on MAS and high-power ^{1}H decoupling techniques, on acetone/SiO_2 samples with a range of surface coverages over a range of temperatures. Both $^1H \rightarrow {}^{13}C$ cross polarization (CP) and direct polarization (DP, no CP, just ^{13}C spin−lattice relaxation) modes were employed. A variety of relaxation measurements were carried out, and the results were interpreted in terms of a simple two-site exchange model. Values of ΔS and ΔH for the formation of the hydrogen-bonded complex were determined.

Experimental Section

Samples. The silica gel used was a high-purity silica (Fisher Scientific S-679) prepared by precipitation, having a particle size distribution from 75 to 150 μm, a surface area (N_2 BET) of 456 m^2/g, an average pore diameter of 30 Å, and a total pore volume of 0.32 cm^3/g. Unless indicated otherwise, the silica samples were initially dehydrated at 150 °C and 10^{-3} Torr (with

10.1021/jp990912r CCC: $18.00
Published on Web 07/30/1999

stirring) for 15 h, a procedure that typically caused a weight reduction of about 4−5%. Deuterium-exchanged silica (referred to here as SiO_2(d)) was prepared by stirring a sample of 3.0 g with 10 cm^3 of 99.9% D_2O (Cambridge Isotopes) under dry N_2(g) at 25 °C for 20 min, removing the supernatant liquid, and repeating the process eight times prior to drying at 10^{-3} Torr and 150 °C for 15 h.

The acetone samples employed were (a) natural-abundance acetone (Mallinckrodt AR, Spectrometric Grade, 99.5% purity, <0.5% H_2O), (b) perdeuterioacetone (acetone-d_6 99.9% ^2H, 0.01% H_2O, Cambridge Isotopes), acetone-1,2,3-^{13}C (99% ^{13}C and <0.02% H_2O, Cambridge Isotopes), acetone-2-^{13}C (99% ^{13}C, <0.02% H_2O, Cambridge Isotopes), and acetone-1-^{13}C (95%, <0.5% H_2O, synthesized here). The acetone-1-^{13}C was synthesized, using a modification of a procedure reported for a different ketone,[30] by the preparation of $^{13}CH_3MgI$ from commercially available $^{13}CH_3I$ (Cambridge Isotopes), conversion of the Grignard reagent to $(^{13}CH_3)_2Cd$ by treatment with $CdCl_2$, and conversion of the labeled dimethyl cadmium to $^{13}CH_3C(O)CH_3$ by treatment with CH_3COCl; details are described elsewhere. The natural-abundance acetone was dried over 3A molecular sieves and then stirred for 24 h and distilled (55 °C, 638 Torr) over boric anhydride (Mallinckrodt AR). Di-*tert*-butyl ketone (2,2,4,4-tetramethylpentan-3-one) was obtained from Aldrich (99% purity, <0.5% H_2O). All H_2O contents were determined by ^1H NMR. All acetone/SiO_2 samples were prepared via adsorption from the gas phase on a vacuum line. Final coverages were determined gravimetrically. All sample transfers, including loading of the MAS rotors (with multi-grooved inserts to seal out moisture), were carried out in a dry-N_2 glovebox.

NMR Experiments. ^{13}C NMR spectra were obtained at 22.7 or 25.3 MHz on a Chemagnetics M-100/90s spectrometer or on a home-built 100 MHz (^1H frequency) spectrometer, respectively, using 7 mm (o.d.) rotors containing 220−250 mg of sample. Both spectrometers used ^1H field strengths of 50 kHz. Dry N_2(g) was used as the MAS drive and bearing gas to help isolate the sample from moisture. In T_2' measurements, the spinning rate was controlled (for synchronization with π pulses) via a rotor tachometer. ^{29}Si NMR spectra were obtained at 17.0 MHz with the Chemagnetics M-100/90S spectrometer. Values of T_1^H, T_1^C, T_1^{Si}, $T_{1\rho}^H$, T_2^C, and T_{CH} were obtained by well-established techniques.[31−33] Values of the proton spin−lattice relaxation time ($T_{1\rho}^H$) in the rotating frame of the applied radio frequency field were measured independently of $^1H-^{13}C$ cross-polarization dynamics by varying the duration of a ^1H spin-lock period prior to a fixed $^1H-^{13}C$ cross-polarization contact time period;[33] the $^1H-^{13}C$ cross-polarization contact time in this experiment was 10 ms for the acetone/SiO_2 samples. Values of $T_{1\rho}^H$ were also measured in an analogous manner via ^{29}Si CP-MAS; the $^1H-^{29}Si$ cross-polarization contact time in this experiment was 2 ms for acetone/SiO_2, dehydrated SiO_2, and untreated SiO_2 samples. Measurements of the laboratory-frame proton spin−lattice relaxation time (T_1^H) and the carbon spin−lattice relaxation time (T_1^C) of acetone/SiO_2 samples were made by inversion−recovery techniques with detection of the ^{13}C CP-MAS intensity that is cross-polarized from protons. The proton spin−lattice relaxation times (T_1^H) of acetone/SiO_2, dehydrated SiO_2, and untreated SiO_2 samples were also measured by an analogous ^{29}Si CP-MAS inversion−recovery approach, with detection of the ^{29}Si CP-MAS intensity that is cross-polarized from protons.[31] The $^1H-^{13}C$ cross-polarization time constants (T_{CH}) of acetone/SiO_2 samples were determined by analysis of variable contact time experiments,[32] using the independently determined $T_{1\rho}^H$ values in a nonlinear least-squares fit of the variable contact time data. $^1H-^{13}C$ dipolar dephasing time constants (T_2's) were obtained by dipolar dephasing (interrupted decoupling) experiments, synchronizing the π pulses with the rotor period. The sample temperature of the CP-MAS probe was calibrated with respect to the reading of the Chemagnetics variable-temperature apparatus on the basis of observing the ^{13}C chemical shift of the chelating carboxyl carbon of samarium acetate hydrate according to the method of Haw and Speed.[34] Relaxation measurements (T_1^C, T_1^H, $T_{1\rho}^H$) on gas-phase acetone samples were made at 22.5 MHz (^{13}C) and 90 MHz (^1H) on a sample of acetone at 25 °C at a pressure of ~300 Torr, where no liquid phase was present; standard relaxation techniques were employed.

Results and Discussion

State of the Acetone/SiO_2 System. During the adsorption of acetone on silica gel, the acetone is present in both the gaseous and adsorbed states, which ultimately reaches equilibrium. During the NMR experiments, this equilibrium is reestablished with gaseous acetone occupying the small, yet macroscopic, void spaces in the sample. Assuming that this void space is 10% or less of the total sample volume, one can readily conclude from a simple calculation that the fraction of acetone in the gas phase in these acetone/SiO_2 samples is essentially negligible (<~0.01%, the exact number depending on the loading level and the temperature). Since no separate gas-phase signals are seen in the ^{13}C NMR spectra, the peaks that are detected are either (a) devoid of a gas-phase contribution (slow exchange with an undetected gaseous component) or (b) weighted-average peaks according to a fast-exchange equation of the following type, for some measured or derived parameter λ:

$$\lambda_{obs} = \frac{N_g}{N_a}\lambda_g + \sum_i \frac{N_i}{N_a}\lambda_i \qquad (1)$$

where N_g is the number of acetone molecules in the void-space gas phase, N_i is the number of acetone molecules in the ith form of a condensed (or adsorbed) phase (summed over all forms of acetone in the condensed phase), and N_a is the total number of acetone molecules in the sample in all forms.

For the fast-exchange case (b), the gaseous component could make a significant contribution to the observed NMR parameter λ_{obs} only if the product of the mole fraction in the gas phase (N_g/N_a) with the gas-phase parameter λ_g is a significant fraction of λ_{obs}. With, as indicated above, the gas-phase mole fraction being so small (<~0.01%), the corresponding value of (N_g/N_a)λ_g can be significant only if λ_g is *dramatically* different from the λ_i values. To check this point, we determined values of the ^{13}C chemical shift, T_1^C, T_1^H, and $T_{1\rho}^H$ of the carbonyl carbon peak in gas-phase acetone at its equilibrium vapor pressure at 25 °C. The observed values (198 ppm, 0.012, 0.58, and 0.035 s, respectively) are not so far from the values measured for the acetone/SiO_2 samples (vide infra) that such gas-phase contributions would be significant in eq 1; hence, such contributions are not considered further below. Thus, the ^{13}C NMR spectra observed in the acetone/SiO_2 samples of this study represent the *adsorbed* state, which itself involves both hydrogen-bonding and non-hydrogen-bonding sites (vide infra).

Another major issue regarding the "global" state of acetone in the acetone/SiO_2 samples of this study is mobility. The fact that earlier ^{13}C NMR studies were based on experiments in which solid-state line-narrowing techniques were not used,[22−25]

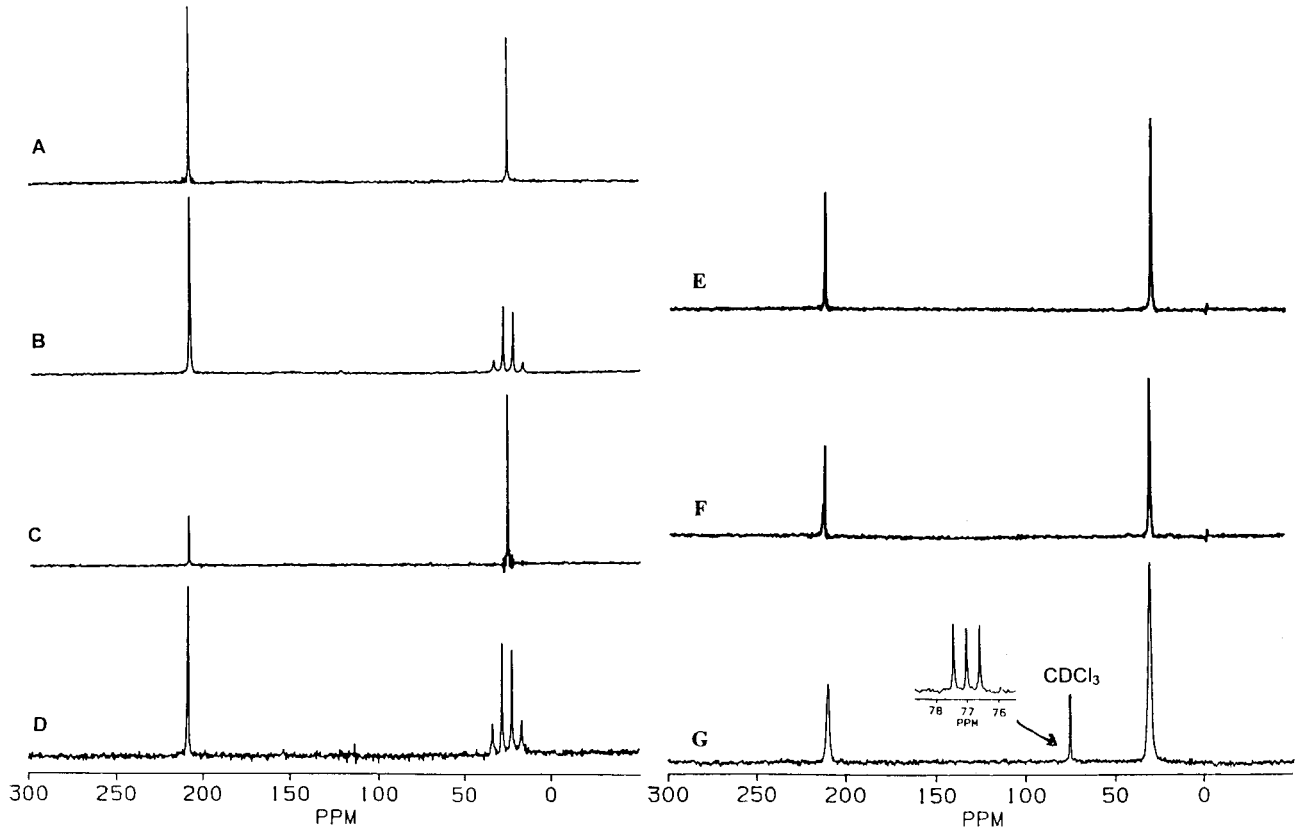

Figure 1. ^{13}C NMR spectra (25 °C) of acetone/SiO_2, with $\theta = 0.80$ (A−D) and $\theta = 0.20$ (E−G): (A) DP-MAS with ^1H dec, 3000 scans, 2 s repetition delay; (B) DP-MAS without ^1H dec, 12 000 scans, 2 s repetition delay; (C) CP-MAS with ^1H dec, 3000 scans, 2 s repetition delay, 40 ms CP contact time; (D) CP-MAS without ^1H dec, 12 000 scans, 2 s repetition delay, 40 ms CP contact time. (E) 2.5 kHz DP-MAS, with 400 repetitions and 3 s delays; (F) 250 Hz DP-MAS, with 400 repetitions and 3 s repetition delays; (G) non-MAS (DP) at 75.5 MHz ^{13}C with 1000 repetitions and 3 s repetition delays, obtained with an acetone/SiO_2 sample was sealed in a 2 mm glass tube and was suspended in a 5 mm NMR tube with $CDCl_3$ in it.

and yet spectra of reasonable quality were obtained, implies that at least a major component of the acetone/SiO_2 system manifests almost liquidlike mobility. The ^{13}C NMR spectra given in Figure 1 indicate that in fact the entire quantity of acetone in these samples is in a state of high mobility, at least in a time-average sense and at least at 25 °C. Figure 1 shows ^{13}C spectra obtained on a natural-abundance acetone/SiO_2 sample with a loading level of 94 mg acetone/1 g SiO_2 (corresponding to a surface coverage, θ, of 0.80, if one assumes an area requirement of 0.38 nm^2/acetone), using DP-MAS (A, B) and CP-MAS (C, D) techniques with (A, C) and without (B, D) high-power ^1H decoupling. In comparing A with C or B with D, one sees spectra of roughly similar quality for CP and DP cases, although with somewhat different relative peak intensities, which reflect details of the relevant relaxation processes. The spectra obtained without ^1H decoupling (B, D) have somewhat larger line widths and display the CH_3 quartet due to $^1H-^{13}C$ J coupling. The somewhat larger line widths in the absence of ^1H decoupling imply the presence of residual dipolar interactions, reflecting a nonliquidlike character in these acetone molecules. Analogous results, albeit with lower signal-to-noise ratio (S/N), are seen in the CP-MAS and DP-MAS spectra obtained in a similar manner, with or without high-power ^1H decoupling, on a sample with a loading level of 23 mg/g ($\theta = 0.20$) (not shown here).[35]

Parts E−G of Figure 1 show ^{13}C DP-MAS spectra obtained on a natural-abundance acetone/SiO_2($\theta = 0.20$) sample obtained with ^1H decoupling and with three different MAS speeds, 2.5, 0.25, and 0 kHz. One sees essentially no difference between the 2.5 and 0.25 kHz spectra, and significantly broader, yet well defined, peaks in the spectrum obtained in the absence of MAS (obtained on a higher field, liquid sample spectrometer configuration, with lower power ^1H decoupling, to eliminate line broadening due to questionable $\mathbf{B}_0$ homogeneity with a typical MAS configuration). The fact that no spinning sidebands are seen in the 0.25 kHz MAS spectrum (F), especially for the carbonyl peak, and the absence in Figure 1G of broad patterns due to the chemical shift anisotropy (CSA) (especially for the carbonyl resonance) or ^1H-dipolar interactions (especially for the methyl resonance) in the static sample spectrum shows that the acetone molecules in this acetone/SiO_2($\theta = 0.20$) sample are substantially liquidlike in terms of overall mobility. The line narrowing brought about by MAS, even at 0.25 kHz, is probably due to the substantial averaging by MAS of $\mathbf{B}_0$ inhomogeneities inherent in the heterogeneous acetone/SiO_2 sample.

The fact that comparable ^{13}C MAS spectra are obtained on the acetone/SiO_2 system via CP and DP approaches signifies a system with substantial mobility, i.e., substantial spectral density of the $^{13}C-^1H$ dipolar interaction in the tens of megahertz range, yielding reasonably efficient spin−lattice relaxation, yet with sufficient spectral density components of the $^{13}C-^1H$ dipole−dipole interaction in the kilohertz range to yield usable $^1H-^{13}C$ CP efficiency.[36] The chemical shifts seen in Figure 1 ($\delta_{CO} = 213.6$ ppm, $\delta_{CH_3} = 29.3$ ppm for $\theta = 0.80$; $\delta_{CO} = 216.8$ ppm, $\delta_{CH_3} = 29.0$ ppm for $\theta = 0.20$) reveal a substantially smaller shielding of the carbonyl carbon in acetone/SiO_2 systems than observed in pure liquid acetone ($\delta_{CO} = 206.7$ ppm, $\delta_{CH_3} = 30.6$ ppm). This effect is consistent with the existence of a hydrogen-bonded complex of acetone when adsorbed on silica, an interpretation that had been used previously,[22−25] in analogy

to low-shielding hydrogen-bonding shifts of the carbonyl group that had been reported earlier.[7,8] Thus, a working hypothesis of the acetone/SiO_2 system is that of a system of acetone moieties rapidly exchanging between the following two states: (a) acetone in a hydrogen-bonded state and (b) acetone in a non-hydrogen-bonded (yet still adsorbed) state. The relative populations of these states will depend on the relevant equilibrium constant(s) and the surface coverage. To examine this dependence, ^{13}C NMR experiments were carried out as a function of surface coverage.

Room Temperature Dependence of Peak Positions on Surface Coverage. ^{13}C CP-MAS and DP-MAS experiments were carried out on acetone/SiO_2 samples at 25 °C in natural abundance for surface coverages ranging from $\theta = 0.10$ to 2.52 (11.6 mg/g to 293.4 mg/g). It is convenient to represent the observed chemical shifts in terms of the carbonyl−methyl chemical shift difference, relative to that in the pure liquid, i.e., $\Delta\delta = (\delta_{CO} - \delta_{CH_3})_{ad} - (\delta_{CO} - \delta_{CH_3})_{liq}$. In the CP-MAS and DP-MAS ^{13}C spectra measured as a function of surface coverage, one finds that the chemical shift of the carbonyl carbon moves dramatically to lower shielding and the chemical shift of the methyl carbon moves slightly (but significantly) to higher shielding as the acetone coverage on the surface is decreased. As the surface coverage is changed from $\theta = 0.10$ to $\theta = 2.52$, the $\Delta\delta$ values range from 12.3 to 2.6 ppm in the DP-MAS results and from 12.3 to 3.1 ppm in the corresponding CP-MAS results. The observed DP-vs-CP differences are almost within the experimental error of these measurements (±0.2 ppm).

The adsorption of acetone on silica gel has been discussed by Bernstein et al.[25] on the basis of a multisite view and modeled on the basis of a two-site (two-state) model involving a single class of strong adsorption. According to this model, nonliquid-like adsorption is accomplished only by hydrogen-bonding between hydroxyl groups of the silica surface (silanols) and the oxygen sites of the carbonyl groups of acetone. We adopt an algebraically similar two-state model as a working hypothesis, with somewhat different definitions of one of the "states". In this model, we refer to the non-hydrogen-bonded, yet adsorbed, acetone as physisorbed acetone, which can be in the first, second, or third, etc., monolayers.

According to this two-state model, we assume that there is an equilibrium among the acetone molecules on the surface, involving adsorption sites (potential hydrogen-bonding surface sites that are not occupied by acetone) and hydrogen-bonded complexes on the surface. This equilibrium is represented by the equation

$$CH_3COCH_3(\text{physisorb}) + \langle Si\rangle OH \overset{K}{\rightleftharpoons} \langle Si\rangle OH\cdots O{=}C(CH_3)_2 \quad (2)$$

(where ⟨Si⟩ represents a silicon atom on the silica surface), from which follows the relationship

$$K = \frac{N_{hb}}{(N_a - N_{hb})(N_s - N_{hb})} \quad (3)$$

where the total number of silanol adsorption sites (per nm^2) is N_s, the number of hydrogen-bonded complexes (per nm^2) is N_{hb}, and the total number of acetone molecules (per nm^2) present (hydrogen-bonded or non-hydrogen-bonded) is N_a. Equation 3 and most of the equations that follow have exactly the same algebraic forms as presented by Bernstein and co-workers for their model.[25]

$\Delta\delta_{hb}$ is defined as the chemical shift difference between the carbonyl and methyl carbons of hydrogen-bonded acetone on an adsorption site relative to the corresponding chemical shift difference of pure liquid acetone, i.e., $\Delta\delta_{hb} = (\delta_{C=0} - \delta_{CH_3})_{hb} - (\delta_{C=0} - \delta_{CH_3})_{liq}$, and $\Delta\delta_{nh}$ represents the chemical shift difference between the carbonyl and methyl carbons of non-hydrogen-bonded (physisorbed) acetone on the surface relative to the corresponding chemical shift difference of pure liquid acetone, i.e., $\Delta\delta_{nh} = ((\delta_{C=0} - \delta_{CH_3})_{nh} - (\delta_{C=0} - \delta_{CH_3})_{liq}$. Because physisorption arises from the attractive forces between nonreacting and non-hydrogen-bonded molecules, i.e., van der Waals forces (e.g., dispersion forces and electric dipole forces), the chemical properties of physisorbed molecules are not changed dramatically from those of molecules of the liquid state. Also, according to the fact that the chemical shift difference ($\Delta\delta$) of acetone/SiO_2 relative to that of pure acetone decreases as the surface coverage is increased, it may be assumed that the chemical shifts of non-hydrogen-bonded acetone are essentially the same (within experimental error) as the corresponding chemical shifts of pure liquid acetone; i.e., $\Delta\delta_{nh} = 0$. Then, for the case of fast chemical exchange

$$\Delta\delta = \frac{N_{hb}}{N_a} \times \Delta\delta_{hb} \quad (4)$$

From eqs 3 and 4, one finds

$$\frac{\Delta\delta}{\Delta\delta_{nh}} = KN_s\left(1 - \frac{\Delta\delta}{\Delta\delta_{nh}}\right) + KN_a\left(\frac{\Delta\delta}{\Delta\delta_{hb}}\right)^2 - KN_a\left(\frac{\Delta\delta}{\Delta\delta_{hb}}\right) \quad (5)$$

By rearranging eq 5, one can obtain

$$\frac{\Delta\delta_{hb}}{\Delta\delta} = \frac{KN_s + 1}{KN_s} + \frac{1}{N_s}N_a\left(1 - \frac{\Delta\delta}{\Delta\delta_{hb}}\right) \quad (6)$$

Equation 6 suggests that a plot of $\Delta\delta_{hb}/\Delta\delta$ against $N_a(1 - \Delta\delta/\Delta\delta_{hb})$ should give a straight line with the slope, $1/N_s$, and the intercept $(KN_s + 1)/KN_s$; this relationship involves the unknown fixed parameter $\Delta\delta_{hb}$, as well as the measured variable parameter $\Delta\delta$. Therefore, to analyze the experimental chemical shift difference, $\Delta\delta$, as a function of the surface concentration of adsorbed molecules (N_a), the parameter $\Delta\delta_{hb}$ was varied to find which value(s) yield straight-line plots according to eq 6. The resulting plots (given elsewhere)[35] reveal that the experimental data fit a straight line reasonably well for $\Delta\delta_{hb} = 15$, 16, 17, and 18 ppm. For $\Delta\delta_{hb}$ values outside this range, reasonable fits could not be obtained. On the basis of these $\Delta\delta_{hb}$ values, the following results were obtained: from DP-MAS data, the number of adsorption sites is 1.4−1.6 su/nm^2 (from the slope), and the equilibrium constant, K, is 2.1−2.8 nm^2/su (from the intercept); from CP-MAS data, the number of adsorption sites, N_s, is 1.3−1.5 su/nm^2, and the equilibrium constant, K, is 2.2−3.1 nm^2/su. The symbol "su" represents a structural unit, i.e., an adsorption site, physisorbed acetone, hydrogen-bonded acetone, or hydrogen-bonding SiO_2 sites. These results are comparable to previously reported results.[24,25]

To further refine the parameters that represent the two-state (physisorbed acetone and hydrogen-bonded acetone) model, the range of $\Delta\delta_{hb}$, N_s, and K values derived from the fit to eq 6 were examined iteratively in terms of eqs 3 and 4 to obtain theoretical curves to compare with the experimental $\Delta\delta$-vs-θ data. The iteration of $\Delta\delta_{hb}$, N_s, and K values began in each case at the average values of the $\Delta\delta_{hb}$, N_s, and K ranges given above from analysis in terms of eq 6. An example of these kinds of iterations and fits is seen in Figure 2A, where $\Delta\delta$ is examined

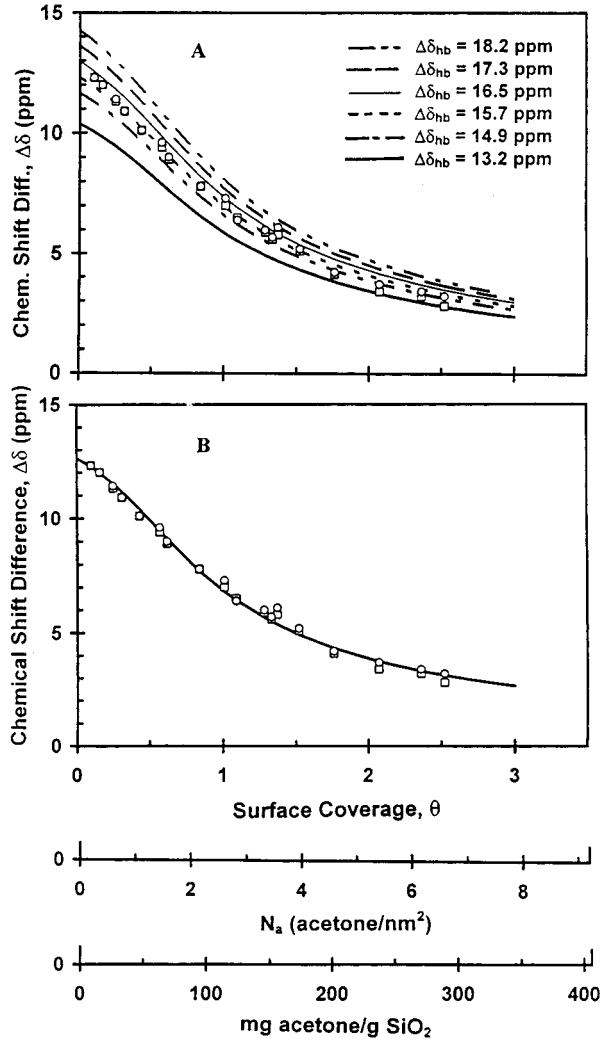

Figure 2. Plots of the (25 °C) chemical shift difference, $\Delta\delta$, between the methyl and carbonyl peaks of acetone/SiO_2 relative to that of pure acetone as a function of surface coverage obtained by CP-MAS experiments (○) and DP-MAS experiments (□). (A) Lines: theoretical fit according to eq 3 and eq 4 with $\Delta\delta_{hb}$ = 16.5, 16.5 ± 5%, ± 10%, ± 20% ppm, N_s = 1.5 sites/nm^2, and K = 2.5 nm^2/su. θ estimated on the basis that θ = 1 corresponds to 2.6 acetones/nm^2. (B) Line (—): theoretical fit according to eq 3 and eq 4 with $\Delta\delta_{hb}$ = 15.2 ppm, N_s = 1.5 sites/nm^2, and K = 3.0 nm^2/su. θ estimated on the basis that θ = 1 corresponds to 2.6 acetones/nm^2.

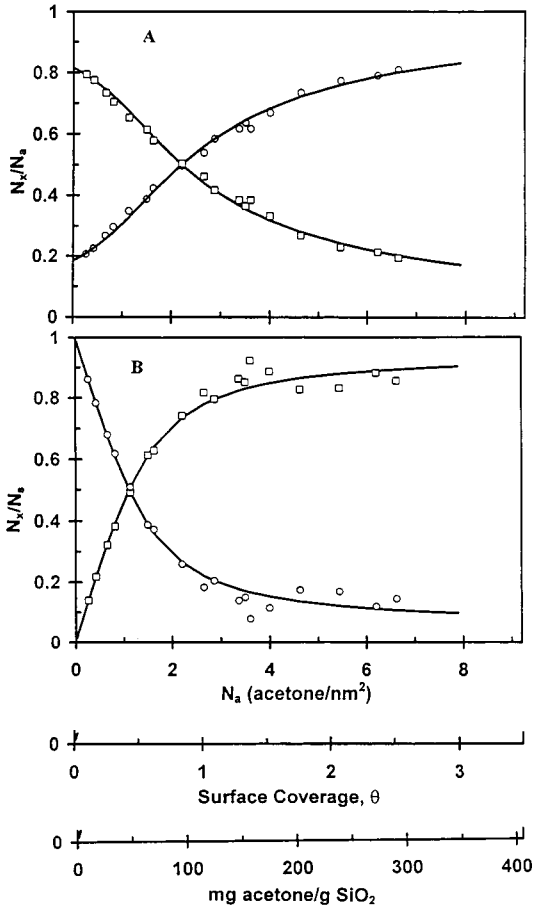

Figure 3. (A) Plots of the (25 °C) fraction of hydrogen-bonded acetone (N_{hb}/N_a) and the fraction of non-hydrogen-bonded acetone ($1 - N_{hb}/N_a$) vs the total number of acetone molecules/nm^2 (N_a) in the acetone/SiO_2 system: points ((□) for N_{hb}/N_a and (○) for $1 - N_{hb}/N_a$), obtained from chemical shift measurements according to eq 4. Line (—): theoretical curve according to eq 3. (B) Plots of the (25 °C) fraction of hydrogen-bonding surface sites (silanols) that are occupied (N_{hb}/N_s) and the fraction of hydrogen-bonding surface sites that are unoccupied ($1 - N_{hb}/N_s$) vs the total number (N_a) of acetone molecules/nm^2 in the acetone/SiO_2 system: points ((□) for N_{hb}/N_s and (○) for $1 - N_{hb}/N_s$) obtained from chemical shift measurements according to eq 4. Line (—): theoretical curve according to eq 3.

explicitly. From a series of such attempted fits, in which $\Delta\delta_{hb}$, N_s, and K were varied systematically, it was found that the best fits to the experimental data were obtained with $\Delta\delta_{hb}$ = 15.2 ppm, N_s = 1.5 sites/nm^2, and K = 3.0 nm^2/su. Figure 2B shows that the theoretical line computed for this parameter set fits the experimental data well. This indicates that the two-state model works well for the acetone/SiO_2 system and that the derived parameters ($\Delta\delta_{hb}$, N_s, and K) can represent the acetone/SiO_2 system.

To further examine these results for $\Delta\delta_{hb}$, N_s, and K, plots of the fraction of acetone that is hydrogen-bonded (N_{hb}/N_a) or non-hydrogen-bonded ($1 - N_{hb}/N_a$) vs the total surface concentration of acetone (N_a) on the silica are shown in Figure 3A. The computed values of N_{hb}/N_s in Figure 3A were derived from eq 4 with N_s = 1.5 sites/nm^2 and K = 3.0 nm^2/su; N_a values for which experimental data were obtained are indicated by the symbol (□) in Figure 3A. Figure 3B gives corresponding plots of the fractions of hydrogen-bonding surface sites (silanols) that are occupied (N_{hb}/n_s) or unoccupied ($1 - N_{hb}/N_s$) vs the total surface concentration of acetone (N_a) on the silica.

If the acetone molecules in the first monolayer are packed with the same density as in the liquid, there would be space for four acetone molecules per nm^2 of silica surface. In general, on a fully hydroxylated silica gel surface (pretreated at 150 °C under vacuum), there are about 5 OH/nm^2.[1-3] Also, on a fully hydroxylated silica gel surface (heated at 25−150 °C under vacuum), such as the silica employed in this study, about 50% of the silanols are isolated silanols (non-hydrogen-bonded) and about 50% of the silanols are hydrogen-bonded silanols (the silanols which are hydrogen-bonded with other silanols).[37,38] That is, there are about 2.5 isolated (non-hydrogen-bonded) silanol OH groups/nm^2 on a fully hydroxylated silica gel surface. In the acetone/SiO_2 system, the surface packing density of hydrogen-bonded acetone is less than 1/2 of the corresponding density in liquid acetone, and only about 1/3 of the individual hydroxyl groups in the acetone/SiO_2 system seem able to interact with an acetone molecule; that is, $N_s \approx 1/3$ (5 OH/nm^2). Only about 3/5 of the non-hydrogen-bonded hydroxyl groups in the acetone/SiO_2 system interact with an acetone molecule; that is, $N_s \approx {}^3/_5$ (2.5 isolated OH/nm^2). Thus, it seems that the

TABLE 1: Measured Relaxation Parameters vs Surface Coverage

coverage, θ	C═O peak	CH_3 peak
	T_1^C (s)[a]	
1.5	3.6	1.3
0.80	2.3	1.1
0.20	1.5	0.76
	T_1^H (s)[b]	
1.5	0.46	0.48
0.80	0.32	0.34
0.20	0.29	0.30
	$T_{1\rho}^H$ (ms)[c]	
1.5	37	33
0.80	33	30
0.20	31	29
	T_{CH} (ms)[d]	
1.5	17	12
0.80	15	10
0.20	9.6	6.7

[a] Obtained from T_1^C inversion−recovery data. Estimated error, ±0.1 s. [b] Obtained from T_1^H (CP) inversion−recovery data. Estimated error, ±0.02 s. [c] Obtained from CP variable-spin-lock data. Estimated error, ±3 ms. [d] Obtained from variable contact time CP data. Estimated error, ±1 ms.

adsorption of acetone on silica gel takes place at well defined sites and that a molecule on one of these sites blocks a certain number of possible neighboring adsorption sites from being occupied by other acetone molecules. In other words, not all the hydroxyl groups on the silica gel surface can interact with acetone molecules, presumably because of steric reasons.

Room-Temperature Relaxation Studies

***T_1^C* Results.** T_1^C values of the methyl and carbonyl carbons of the acetone/SiO_2 system were measured for three acetone loading levels ($\theta = 0.20$, 0.80, and 1.5) by the ^{13}C T_1 inversion−recovery experiment that is based on CP-generated ^{13}C magnetization. In these experiments, the relaxation−recovery time (τ) was varied from 10 μs to 20 s, revealing that for each sample a single-exponential relaxation behavior is present for carbonyl groups and a single-exponential relaxation behavior is present for methyl groups. The T_1 values derived from the least-squares plots (not shown here)[35] are given in Table 1.

As one can see from Table 1, the T_1^C values detected for the methyl and carbonyl carbons of acetone/SiO_2($\theta = 1.5$) are 1.3 and 3.6 s, respectively, T_1^C values of acetone/SiO_2($\theta = 0.80$) are 1.1 and 2.3 s, respectively, and T_1^C values of acetone/SiO_2($\theta = 0.20$) are 0.76 and 1.5, respectively. The T_1^C value of the carbonyl carbons is larger than that of the methyl carbons at each surface coverage, presumably because methyl carbons are closer to protons than are carbonyl carbons. T_1^C values of both methyl and carbonyl carbons of acetone decrease as the acetone surface coverage is decreased.

The fact that only one relaxation component was observed for each carbon peak at each surface coverage means that there is a fast chemical exchange, presumably between mobile and immobile species. The observed T_1^C value is the time (motion/exchange) averaged spin−lattice relaxation time of the different species. As the acetone surface coverage is increased, the average mobility of acetone is expected to become greater, since a larger fraction of the acetone is non-hydrogen-bonded at high surface coverage. This should cause the averaged T_1^C value to become larger, assuming that the molecular motion of the mobile (non-hydrogen-bonded) species has an inverse correlation time τ_c^{-1} that is larger than the ^{13}C Larmor frequency of 22.7 MHz[35,39−45] so that it relaxes more slowly than does the hydrogen-bonded species. A system, such as acetone in this non-hydrogen-bonded state, where faster motion leads to a larger T_1 value, is often referred to as being in the "motional narrowing limit".

Since the observed T_1^C values are the time (motion/exchange) averaged spin−lattice relaxation times of the various species, the observed T_1^C values are dependent on surface coverage. By examining the experimentally observed T_1^C values as a function of surface coverage, one can estimate individual T_1^C values for hydrogen-bonded acetone and non-hydrogen-bonded acetone.

With the two-site (two-state) model consisting of hydrogen-bonded acetone and non-hydrogen-bonded acetone adsorbed on the silica surface, in a condition of fast exchange, as described above, one can describe the dependence of the "generic" relaxation time T_i on surface coverage in terms of the following version of eq 1 (for $\lambda_i = 1/T_i$):

$$\frac{1}{T_i} = \frac{\frac{1}{T_{i\mathrm{hb}}}N_{\mathrm{hb}} + \frac{1}{T_{i\mathrm{nh}}}(N_{\mathrm{a}} - N_{\mathrm{hb}})}{N_{\mathrm{a}}} \tag{7}$$

Rearranging the above equation,

$$\frac{1}{T_i} = \frac{1}{T_{i\mathrm{nh}}} + \left(\frac{1}{T_{i\mathrm{hb}}} - \frac{1}{T_{i\mathrm{nh}}}\right)\frac{N_{\mathrm{hb}}}{N_{\mathrm{a}}} \tag{7′}$$

and substituting eq 4 into eq 7′ yields

$$\frac{1}{T_i} = \frac{1}{T_{i\mathrm{nh}}} + \left(\frac{1}{T_{i\mathrm{hb}}} - \frac{1}{T_{i\mathrm{nh}}}\right)\frac{\Delta\delta}{\Delta\delta_{\mathrm{hb}}} \tag{8}$$

From eq 8, we expect that a plot of $1/T_i$ vs $\Delta\delta/\Delta\delta_{\mathrm{hb}}$ should give a straight line with the intercept of $1/T_{i\mathrm{nh}}$ and a slope of $(1/T_{i\mathrm{hb}} - 1/T_{i\mathrm{nh}})$.

Figure 4A shows three-point plots of the experimental, $1/T_1^C$ values against $\Delta\delta/\Delta\delta_{\mathrm{hb}} = N_{\mathrm{hb}}/N_{\mathrm{a}}$ for the methyl and carbonyl carbons of acetone/SiO_2 samples with surface coverages of 1.5, 0.80, and 0.20; also shown are the computer-based least-squares fit to eq 8. The T_1^C values derived for the methyl and carbonyl carbons of hydrogen-bonded acetone, which are listed in Table 2, are 0.65 and 1.45 s, respectively, and are 3.6 and >100 s, respectively, for non-hydrogen-bonded acetone, larger for the methyl and carbonyl carbons of non-hydrogen-bonded acetone than for hydrogen-bonded acetone. This is because molecular motion of non-hydrogen-bonded acetone is faster (larger τ_c^{-1}) than the ^{13}C Larmor frequency of 22.7 MHz, so the ^{13}C nuclei of this species relax more slowly than does the corresponding ^{13}C magnetization of hydrogen-bonded acetone. The T_1^C values of non-hydrogen-bonding acetone are roughly of the same general magnitude as those of liquid acetone, which are typically 25 and 36 s, respectively, at room temperature. This indicates that non-hydrogen-bonded acetone in the acetone/SiO_2 system is rather "liquid-like". The carbonyl carbon has no directly attached hydrogens, so $^{13}C-^1H$ dipolar interactions and relaxation effects are much weaker than for methyl carbons.

***T_1^H* Results.** T_1^H values, as monitored at the methyl and carbonyl carbons of acetone/SiO_2 samples ($\theta = 1.5$, 0.80, and 0.20), were measured by the ^1H T_1 inversion−recovery experiments with a ^{13}C-monitored CP approach.[33] In this experiment, the ^1H relaxation−recovery time, t, was varied from 50 μs to 5 s. The T_1^H values extracted from computer fits (not shown here)[35] of the data for these acetone/SiO_2 samples are listed in Table 1. These results reveal a single proton spin−lattice relaxation behavior for each ^{13}C peak for each sample. The T_1^H

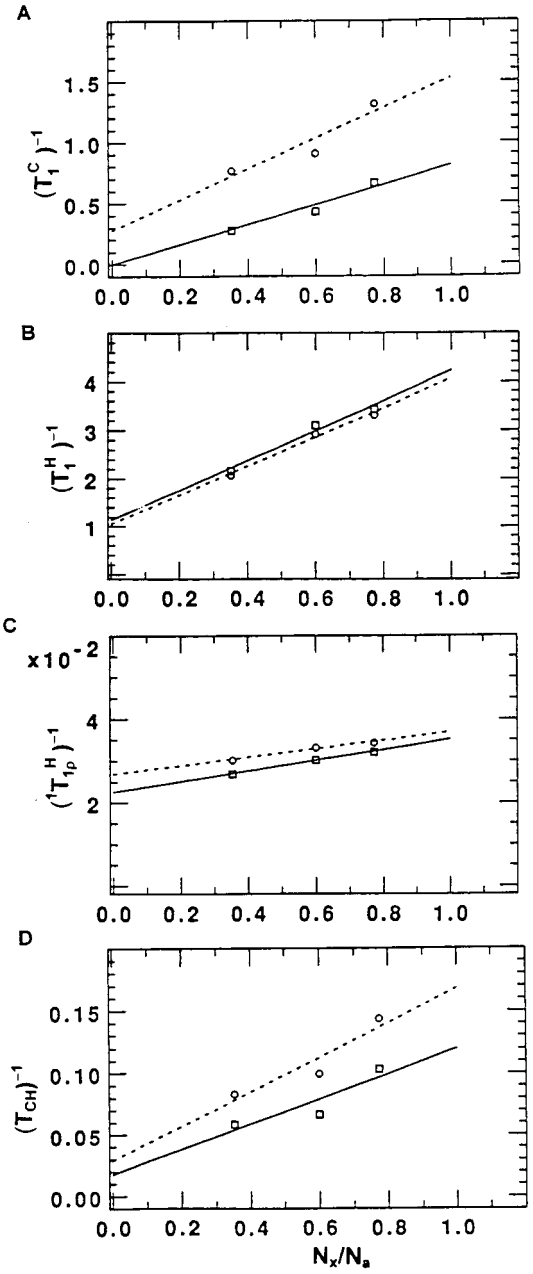

Figure 4. Plots of T_i^{-1} for methyl (○) and carbonyl (□) peaks of acetone/SiO_2 as functions of a measure of surface coverage, according to eq 8 for (A) T_1^C, (B) T_1^H, (C) $T_{1\rho}^H$, and (D) T_{CH} at 25 °C.

values detected via methyl and carbonyl carbons of acetone/SiO_2($\theta = 1.5$) are 0.48 and 0.46 s, respectively; the corresponding T_1^H values of acetone/SiO_2($\theta = 0.80$) are 0.34 and 0.32 s, respectively; and the T_1^H values of acetone/SiO_2($\theta = 0.20$) are 0.30 and 0.29 s, respectively. There are no statistically significant differences ($\pm\sim$0.03 s) between the methyl and carbonyl carbon values for each of these three samples, implying that both the methyl and carbonyl carbons rely upon the same set of ^1H spins for cross polarization (at least on the time scale of $^1H-^{13}C$ CP). Since only one proton relaxation component was observed via each carbon peak at each surface coverage and since the T_1^H value depends on the acetone surface coverage, there is apparently fast chemical exchange between mobile (non-hydrogen-bonded) and immobile (hydrogen-bonded) species, yielding the time (motion/exchange) averaged spin−lattice relaxation behavior of the species of different mobility. As the acetone surface coverage is increased, the average motion of acetone becomes faster, because a larger fraction of acetone is non-hydrogen-bonded. This should cause the average T_1^H value to become larger, assuming that the molecular motion of the mobile (non-hydrogen-bonded) species has a τ_C^{-1} that is much larger than the ^1H Larmor frequency of 90 MHz, so it relaxes more slowly than does the hydrogen-bonded species.

TABLE 2: Relaxation Parameters for Hydrogen-Bonded and Non-Hydrogen-Bonded Acetone

type of acetone	C=O peak	CH_3 peak
	T_1^C (s)[a]	
non-hydrogen-bonded	>100	3.6
hydrogen-bonded	1.45	0.65
	T_1^H (s)[b]	
non-hydrogen-bonded	0.88	0.95
hydrogen-bonded	0.24	0.25
	$T_{1\rho}^H$ (ms)[c]	
non-hydrogen-bonded	44	37
hydrogen-bonded	28	27
	T_{CH} (ms)[d]	
non-hydrogen-bonded	57	35
hydrogen-bonded	8.3	5.9

[a] Obtained from fitting measured T_1^C values to eq 8. Estimated error, ±10%. [b] Obtained from fitting measured T_1^H values to eq 8. Estimated error, ±0.02 s. [c] Obtained from fitting measured $T_{1\rho}^H$ values to eq 8. Estimated error, ±3 ms. [d] Obtained from fitting measured T_{CH} values to eq 8. Estimated error, ±12%.

In analogy to what was described above for T_1^C values, Figure 4B shows the computer-based least-squares fit of the plot of experimental $1/T_1^H$ values against $\Delta\delta/\Delta\delta_{hb}$ for detection at the methyl and carbonyl carbons of acetone/SiO_2 samples with surface coverages of 1.5, 0.80, and 0.20. The T_1^H values of the methyl and carbonyl carbons of hydrogen-bonded acetone and non-hydrogen-bonded acetone derived from this analysis, which are listed in Table 2, are 0.25 and 0.24 s, respectively, for the methyl and carbonyl carbons of hydrogen-bonded acetone, and those for non-hydrogen-bonded acetone are 0.95 and 0.88 s, respectively. These T_1^H values are larger for non-hydrogen-bonded acetone than the corresponding values of hydrogen-bonded acetone, because molecular motion of non-hydrogen-bonded acetone has a τ_c^{-1} that is much larger than the ^1H Larmor frequency of 90 MHz, so these protons relax more slowly than do the protons of hydrogen-bonded acetone.

***$T_{1\rho}^H$* Measurement by ^{13}C NMR.** The rotating frame proton spin−lattice relaxation time ($T_{1\rho}^H$) can be measured via ^{13}C, using the CP-MAS variable contact time techniques (vide infra).[32] In addition, an "independent" $T_{1\rho}^H$ measurement based on a fixed value of the CP contact time ($t_{CP} = 10$ ms) and a variable ^1H spin-lock delay period, τ, prior to CP was also used in this study to obtain $T_{1\rho}^H$ values of acetone/SiO_2 samples with three surface coverages ($\theta = 0.20$, 0.80, and 1.5).[33] The $T_{1\rho}^H$ values derived from the relaxation plots for the carbonyl and methyl carbons (not shown here),[35] which are given in Table 1, are 37 and 33 ms, respectively, for acetone/SiO_2($\theta = 1.5$); the corresponding values of acetone/SiO_2($\theta = 0.80$) are 33 and 30 ms, respectively; and the corresponding values of acetone/SiO_2($\theta = 0.20$) are 31 and 29 ms, respectively. At each surface coverage of these acetone/SiO_2 samples, there is no statistically significant difference (±3 ms) between the $T_{1\rho}^H$ behaviors of the methyl and carbonyl carbons, implying that the combination of motion of adsorbed acetone and rotating-frame $^1H-^1H$ spin exchange among various silanol protons and methyl protons is fast enough to establish an equilibrium among the different protons on a time scale of a few milliseconds for these three samples. Specifically, this implies that there is a fast site

exchange between mobile and immobile species, yielding the time average of the rotating-frame spin−lattice relaxation time constants of the species of different mobilities.

As discussed above, as the acetone surface coverage is increased, the time-averaged motion of acetone is expected to become faster, because a larger fraction of acetone is non-hydrogen-bonded. This should cause the average $T_{1\rho}^{H}$ value to become larger, assuming that the molecular motion of the mobile (non-hydrogen-bonded) species has a τ_c^{-1} value that is much larger than the intensity of the radio frequency spin-lock, 50 kHz, so these more mobile species relax more slowly than does hydrogen-bonded acetone.

By analogy to what was discussed above for T_1^C and T_1^H, Figure 4C shows a plot of the experimental values of $1/T_{1\rho}^{H}$ against $\Delta\delta/\Delta\delta_{hb}$ for the methyl and carbonyl carbons of acetone/SiO_2 with surface coverages of 1.5, 0.80, and 0.20. As summarized in Table 2, the $T_{1\rho}^{H}$ values measured at the methyl and carbonyl carbons of hydrogen-bonded acetone, derived from the computer-based least-squares fits, are 27 and 28 ms, respectively, and the corresponding $T_{1\rho}^{H}$ values of non-hydrogen-bonded acetone are 37 and 44 ms, respectively. These $T_{1\rho}^{H}$ values of non-hydrogen-bonded acetone are larger than the corresponding values of hydrogen-bonded acetone, because the τ_c^{-1} value that characterizes molecular motion of non-hydrogen-bonded acetone is much larger than the intensity of the radio frequency spin-lock, 50 kHz, so the protons of these more mobile acetone molecules relax more slowly than do protons of hydrogen-bonded acetone. $T_{1\rho}^{H}$ values also exhibit the same kind of trends as do T_1^C and T_1^H for the acetone/SiO_2 system: (a) an increase in acetone surface coverage leads to an increase in $T_{1\rho}^{H}$ (or T_1^C or T_1^H); (b) only one relaxation parameter was obtained for each carbon peak of each sample; (c) the $T_{1\rho}^{H}$ (or T_1^C or T_1^H) values of the methyl and carbonyl carbons of non-hydrogen-bonded acetone are larger than those of hydrogen-bonded acetone in the acetone/SiO_2 system. Hence, all of these relaxation results are consistent with each other and are governed by an equation of the form represented in eq 1, i.e.,

$$\frac{1}{T_i} = \frac{1}{T_{ihb}}\frac{N_{hb}}{N_a} + \frac{1}{T_{inh}}\frac{(N_a - N_{hb})}{N_a} \qquad (9)$$

where $T_i = T_1^C$, T_1^H, or $T_{1\rho}^{H}$.

Relaxation Studies Based on ^{29}Si NMR. In 1980, Sindorf and Maciel published the first high-resolution example of the use of $^1H \rightarrow X$ cross-polarization for surface-selective observation of nucleus X in a demonstration of $^1H \rightarrow {}^{29}Si$ CP in silica gel.[46] ^{29}Si CP-MAS techniques were utilized in the study reported here to measure a variety of ^{1}H and ^{29}Si relaxation parameters and provide useful information about the surface structure/dynamics of the acetone/SiO_2 system. To avoid the dependence of relaxation behavior in the acetone/SiO_2 system on the strength of the static magnetic field, the ^{29}Si CP-MAS experiments were carried out at the same field as used for the ^{13}C CP-MAS experiments. ^{29}Si-monitored T_1^H and $T_{1\rho}^{H}$ measurements were carried out on acetone/SiO_2 samples ($\theta = 1.5$, 0.80, and 0.20) and, for comparison, on dehydrated SiO_2 and untreated SiO_2.

In the proton inversion−recovery $^1H \rightarrow {}^{29}Si$ CP experiments for measuring T_1^H for each sample, all the ^{1}H magnetization represented in each set of spectra appeared to relax at a common spin−lattice relaxation rate, so the total integrated intensity was fit (not shown here)[35] by computer analysis to an exponential decay equation, as for the T_1^H inversion−recovery ^{13}C CP method, yielding the results summarized in Table 3. The ^{29}Si-detected T_1^H value is 0.44 s for acetone/SiO_2($\theta = 1.5$), 0.33 s for acetone/SiO_2($\theta = 0.80$), 0.28 s for acetone/SiO_2($\theta = 0.20$), 0.40 s for dehydrated SiO_2, and 0.26 s for untreated SiO_2. Comparing the T_1^H values of acetone/SiO_2 samples ($\theta = 1.5$, 0.80, and 0.20) obtained by the ^{13}C−CP approach (Tables 1 and 3) and by the ^{29}Si−CP approach (Table 3), one can see that they are essentially identical for each specific sample and have the same trends: an increase in acetone surface coverage leads to an increase in T_1^H values. The fact that the ^{13}C-detected and ^{29}Si-detected T_1^H values are essentially the same for a given sample is due to a fast ^{1}H spin exchange (presumably $^1H-{}^1H$ flip-flops) between the methyl protons of acetone and silanol protons.

TABLE 3: T_1^H and $T_{1\rho}^{H}$ Obtained by ^{13}C and ^{29}Si CP-MAS

^{13}C CP-MAS Approach		
surface coverage, θ[a]	T_1^H (s)[b]	$T_{1\rho}^{H}$ (ms)[c]
1.5	0.47	35
0.80	0.33	32
0.20	0.29	30
^{29}Si CP-MAS Approach		
surface coverage,θ	T_1^H (s)[d]	$T_{1\rho}^{H}$ (ms)[e]
1.5	0.44	35
0.80	0.33	32
0.20	0.28	30
dehydrated SiO_2	0.40	56
untreated SiO_2	0.26	30

[a] Calculated by assuming that the entire silica surface is covered by one monolayer of acetone molecules, with the "size" of acetone 38 Å^2 and the silica surface area 456 m^2/g. [b] T_1^H values are the average values of the methyl and carbonyl peaks (from Table 1). Estimated error, ±0.02 s. [c] $T_{1\rho}^{H}$ values are the average values of the methyl and carbonyl peaks (from Table 1). Estimated error, ±3 ms. [d] Estimated error, ±0.02 s. [e] Estimated error, ±3 ms.

The T_1^H value of dehydrated SiO_2 is larger than the T_1^H values for the two lower surface coverages of acetone/SiO_2 samples ($\theta = 0.80$ and 0.20) and for untreated SiO_2 because dehydrated SiO_2 lacks both adsorbed acetone and adsorbed water, either of which can serve as a source of relaxation (a relaxation "sink") on the SiO_2 surface. The T_1^H value measured for the acetone/SiO_2($\theta = 1.5$) sample is comparable to (or a little larger than) that of dehydrated SiO_2 because, although this sample does not lack adsorbed acetone (a potential relaxation "sink"), the average molecular motion of acetone is very fast in this system. This greater acetone mobility, due to a larger fraction of acetone that is non-hydrogen-bonded, diminishes the efficiency of proton spin−lattice relaxation. As mentioned above, molecular motion of the mobile species (non-hydrogen-bonded acetone) has a τ_c^{-1} value that is much larger than the ^{1}H Larmor frequency, 90 MHz, so the protons of such species relax more slowly than do protons of hydrogen-bonded species.

Rotating-frame proton spin−lattice relaxation measurements were also measured for the acetone/SiO_2 samples ($\theta = 1.5$, 0.80, and 0.20), dehydrated SiO_2, and untreated SiO_2 via the $^1H \rightarrow {}^{29}Si$ CP approach.[33] The magnetizations of all three silicon sites (peaks) in each sample were found to decay exponentially at rates determined for each sample by a common $T_{1\rho}^{H}$ value, which was obtained by computer fitting the total integrated ^{29}Si intensity to a decaying exponential,[35] as for $T_{1\rho}^{H}$ experiments by the ^{13}C CP approach. The fact that a common $T_{1\rho}^{H}$ value is measured for all three silicon sites in each sample, as represented in Table 3, indicates that the combination of motion of adsorbed acetone (or adsorbed water) and rotating-frame $^1H-{}^1H$ spin diffusion among various protons responsible for $^1H-{}^{29}Si$ CP is

fast enough to establish spin equilibration among the different protons on a time scale of tens of milliseconds for these samples. $T_{1\rho}{}^{H}$ also reflects the difference in hydration level in the silica-only samples; the $T_{1\rho}{}^{H}$ value (30 ms) of untreated SiO_2 is smaller than the $T_{1\rho}{}^{H}$ value (57 ms) of dehydrated SiO_2. $T_{1\rho}{}^{H}$ is essentially the same (33 ± 2 ms) within experimental error for all three acetone/SiO_2 samples ($\theta = 0.20, 0.80, 1.5$). Comparing the $T_{1\rho}{}^{H}$ values of acetone/SiO_2 samples obtained by the ^{29}Si CP approach with those obtained by the ^{13}C CP approach, one can see that they are essentially identical (within experimental error) for a given sample; this fact, and the analogous correspondence of $T_1{}^{H}$ values, are due to the fact that there is a fast ^1H spin exchange (via $^1H-{}^1H$ flip-flops) between the methyl protons and silanol protons in the acetone/SiO_2 system. The $T_{1\rho}{}^{H}$ value of dehydrated SiO_2 is much larger than those of acetone/SiO_2 samples and untreated (partially hydrated) SiO_2 because of the lack of a rotating-frame proton spin−lattice relaxation "sink" provided by adsorbed acetone or water.

Variable Contact Time CP MAS Studies by ^{13}C NMR. A common approach for characterizing ^{13}C CP dynamics (measuring T_{CH} and $T_{1\rho}{}^{H}$) is based on the analysis of variable contact time data in terms of the following equation, which is valid for the case $T_{1\rho}{}^{C} \gg T_{1\rho}{}^{H}$:[32]

$$M(\tau) = \frac{M^*}{1 - \left(\frac{T_{CH}}{T_{1\rho}{}^{H}}\right)}\left[\exp\left(\frac{-\tau}{T_{1\rho}{}^{H}}\right) - \exp\left(\frac{-\tau}{T_{CH}}\right)\right] \qquad (10)$$

In eq 10, τ is the variable CP contact time, $M(\tau)$ is the ^{13}C magnetization generated with a CP contact time of τ, and M^* is the ^{13}C magnetization that would be generated if cross-polarization were infinitely fast (if $T_{CH}{}^{-1}$ were infinite) and rotating-frame spin−lattice relaxation were infinitely slow (if $T_{1\rho}{}^{H}$ were infinite). T_{CH} is the cross-polarization time constant that represents the coupling between the ^{13}C spin reservoir and the ^1H spin reservoir. Other things (i.e., motional effects) being equal, the stronger the $^1H-{}^{13}C$ dipolar interaction, the smaller the T_{CH} value. Since a dipolar interaction depends not only on internuclear distance but also on motion of one or both of the coupled spins, T_{CH} also reflects motion in the spin system.

Variable contact time experiments were carried out on acetone/SiO_2 samples with three surface coverages ($\theta = 1.5$, 0.80, and 0.20). The ^{13}C CP-MAS methyl and carbonyl peak intensities were analyzed by computer fits (not shown here)[35] based on eq 10, using the independently determined $T_{1\rho}{}^{H}$ values (vide supra), yielding the T_{CH} values listed in Table 1. As expected, the carbonyl carbon T_{CH} value given in Table 1 for any one of these samples is larger than that of the methyl carbons, because the carbonyl carbons are more remote from protons than are methyl carbons. For acetone/SiO_2($\theta = 1.5$), the T_{CH} values for methyl and carbonyl carbons are 12 and 17 ms, respectively; for acetone/SiO_2($\theta = 0.80$), the values are 10 and 15 ms, respectively; and for acetone/SiO_2($\theta = 0.20$), 6.7 and 9.6 ms, respectively. These rather large T_{CH} values indicate that the relevant $^1H-{}^{13}C$ dipolar interactions are much weaker (in a time-averaged sense) for the acetone molecules in the acetone/SiO_2 system than in typical, rigid organic solids, presumably because of the great mobility of acetone on the silica surface. A hydrogen-bonded acetone molecule on the silica surface at room temperature may rotate rapidly about the $(CH_3)_2C{=}O\cdots HOSi$ hydrogen-bonding axis, or acetone may jump rapidly from one site to another; both motions would reduce the effective $^1H-{}^{13}C$ dipolar−dipolar interaction.

T_{CH} values of both methyl and carbonyl carbons of acetone in the three acetone/SiO_2 samples are larger for higher acetone surface coverage, presumably because acetone molecules, on average, become more mobile as the surface coverage is increased. This greater average mobility reduces the effective $^1H-{}^{13}C$ dipolar interaction, and T_{CH} becomes larger. The fact that the observed T_{CH} value depends on the surface coverage and that only a single T_{CH} value is observed for each carbon at each surface coverage implies that the observed T_{CH} value is a manifestation of the time (motion) average of the $^1H-{}^{13}C$ dipolar−dipolar interaction. This would seem to mean that there is a fast chemical exchange between the more mobile species and the less mobile species.

In the same fashion as described above for $T_1{}^{C}$, $T_1{}^{H}$, and $T_{1\rho}{}^{H}$ values, Figure 4D shows the computer-based least-squares fit of the plot of experimentally determined $1/T_{CH}$ values against $\Delta\delta/\Delta\delta_{hb}$ for the methyl and carbonyl resonances of acetone/SiO_2 samples with surface coverages of 1.5, 0.80, and 0.20. The T_{CH} values derived from these plots are listed in Table 2 for the methyl and carbonyl carbons of hydrogen-bonded acetone and non-hydrogen-bonded acetone. From this table, one can see that the T_{CH} values of the methyl and carbonyl carbons of hydrogen-bonded acetone are 5.9 and 8.3 ms, respectively, and the corresponding values of non-hydrogen-bonded acetone are 35 and 57 ms, respectively. The T_{CH} values of non-hydrogen-bonded acetone are larger than those of hydrogen-bonded acetone because the fast molecular motion of non-hydrogen-bonded acetone reduces the effective $^1H-{}^{13}C$ dipolar interaction. Thus, T_{CH} exhibits trends that are consistent with those for $T_1{}^{C}$, $T_1{}^{H}$, and $T_{1\rho}{}^{H}$ values of the acetone/SiO_2 system.

^{13}C NMR Studies on Selectively Deuterated Acetone/SiO_2. To better understand spin dynamics in the acetone/SiO_2 system, one would like to know which protons are responsible (primarily or exclusively) for $^1H-{}^{13}C$ cross-polarization. For examining this issue, ^{13}C DP-MAS and CP-MAS NMR experiments were carried out on deuterated acetone adsorbed on the silica surface, acetone-d_6/SiO_2, and on isotopically normal acetone adsorbed on a deuterated silica surface, acetone/SiO_2(d). Figure 5 shows the ^{13}C DP-MAS and DP-MAS NMR spectra of acetone/SiO_2, acetone/SiO_2(d), and acetone-d_6/SiO_2. The experimental conditions (number of repetitions, repetition delay, and contact time) were the same for all three samples in each specific type of experiment. The acetone surface coverage was the same for each of the three samples ($\theta = 1.0$, that is, 2.6 acetone/nm^2 or 117 mg of acetone/g of SiO_2).

In the ^{13}C DP-MAS and CP-MAS NMR spectra of acetone/SiO_2(d)($\theta = 1.0$) (parts C and D of Figure 5, respectively), one can see that the signal intensities of the methyl carbons are comparable in the DP-MAS and CP-MAS spectra, but the signal intensity of carbonyl carbons is smaller in the CP-MAS spectrum than in the DP-MAS spectrum. An important question is whether the relative signal intensity of the carbonyl carbons of acetone/SiO_2(d) is reduced in the CP-MAS experiment because of (a) a lack of the silanol protons of the silica surface, which were part of the spin reservoir serving as a source for $^1H-{}^{13}C$ cross-polarization in the undeuterated sample or (b) because there is some proton−deuterium exchange between protons of methyl groups of adsorbed acetone and deuteriums of silanol groups of the silica surface, reducing the amount of protons of methyl groups available for $^1H-{}^{13}C$ CP. Proton−deuterium exchange between the protons of methyl groups of acetone and deuterium of silanol groups of silica surface could conceivably occur, possibly via an enol intermediate. The fact that the observed DP-MAS and CP-MAS signals of the methyl carbons of acetone/SiO_2(d) are comparable to each other, and to the methyl CP-MAS and DP-MAS signals of acetone/SiO_2, indicates that the

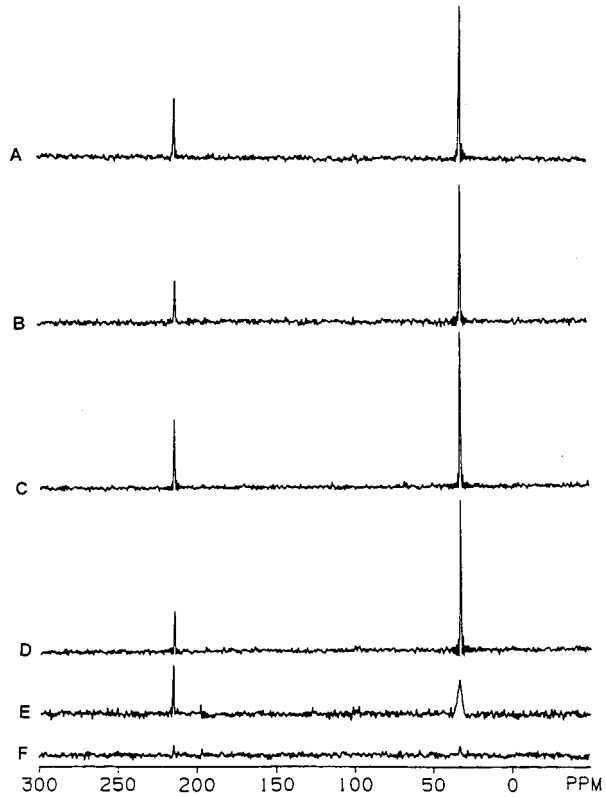

Figure 5. ^{13}C MAS NMR spectra of acetone/SiO_2 samples with the same surface coverage ($\theta = 1.0$) (for DP-MAS, 12 000 repetitions and 3 s repetition delay; and for CP-MAS, 6000 repetitions, 3 s repetition delay and 40 ms contact time): (A) DP-MAS, acetone/SiO_2; (B) CP-MAS, acetone/SiO_2; (C) DP-MAS, acetone/SiO_2(d); (D) CP-MAS, acetone/SiO_2(d); (E) DP-MAS, acetone-d_6/SiO_2; (F) CP-MAS, acetone-d_6/SiO_2. All data taken at 25 °C.

protons of methyl groups dominate the $^1H-^{13}C$ cross-polarization process. Nevertheless, it is not obvious whether the protons of silanol groups of the silica surface participate in the $^1H-^{13}C$ cross-polarization process of the carbonyl carbon of adsorbed acetone.

In the ^{13}C DP-MAS and CP-MAS NMR spectra of acetone-d_6/SiO_2($\theta = 1.0$) (parts E and F of Figure 5, respectively), one can see that there is a sharp peak for the carbonyl carbon and a broad peak for the methyl carbons in the DP-MAS spectrum. The decreased methyl peak height appears to be correlated with the increased line width, which is due to the coupling to deuterium in the $-CD_3$ groups in acetone-d_6/SiO_2. For acetone-d_6, $^{13}C-^2H$ *J*-coupling for the $-CD_3$ group is about 21 Hz, and it splits the $-CD_3$ peak into seven peaks with relative intensities 1:3:6:7:6:3:1. The signal intensities of both carbonyl and methyl carbons are much smaller in the CP-MAS spectrum of acetone-d_6/SiO_2 (Figure 5F). The tiny remaining signal intensities are due to either cross-polarization from protons of silanol groups of the silica surface or from protons of methyl groups of acetone which arise from proton−deuterium exchange between protons of silanol groups and deuteriums of CD_3 groups.

The origin of the weak CP signal seen in Figure 5F was examined by acquiring and comparing the mass spectra of the initial acetone-d_6 and of acetone that had desorbed from the acetone-d_6/SiO_2 sample after adsorption for 10 days. From this comparison, it was concluded that about 30% of the acetone-d_6 had been transformed into acetone-d_5 (i.e., CD_3COCHD_2). That is, about 5% of the methyl deuteriums have been replaced by protons. The fact that the signal intensities of both the carbonyl and methyl carbons are dramatically decreased in the CP-MAS spectrum of acetone-d_6/SiO_2 relative to that of the isotopically normal acetone/SiO_2 sample indicates that the methyl protons of acetone/SiO_2 dominate the $^1H \rightarrow {}^{13}C$ cross-polarization process in acetone/SiO_2. In exploring whether the protons of silanol groups of the silica surface also participate in the $^1H-{}^{13}C$ cross-polarization process, T_{CH} and $T_{1\rho}{}^H$ values of the methyl and carbonyl carbons of acetone/SiO_2, acetone/SiO_2(d) and acetone-d_6/SiO_2 were measured by the same methods described above. The results derived from fitting the variable contact time data of the methyl and carbonyl carbon resonances of acetone/SiO_2, acetone/SiO_2(d), and acetone-d_6/SiO_2 to eq 10 (not given here)[35] with $T_{1\rho}{}^H$ constrained to values determined from fitting the variable spin-lock CP-MAS curves (not shown here)[35] are, for acetone/SiO_2($\theta = 1.0$), T_{CH}(C═O) = 17 ms, $T_{CH}(CH_3)$ = 11 ms, $T_{1\rho}{}^H$(CO) = 30 ms, $T_{1\rho}(CH_3)$ = 29 ms; for acetone/SiO_2(D)($\theta = 1.0$), T_{CH}(C═O) = 14 ms, $T_{CH}(CH_3)$ = 9 ms, $T_{1\rho}{}^H$(C═O) = 32 ms, $T_{1\rho}{}^H(CH_3)$ = 28 ms; for acetone-d_6/SiO_2($\theta = 1.0$), T_{CH}(C═O) = 44 ms, $T_{CH}(CH_3)$ = 34 ms. The $T_{1\rho}{}^H$ experiment was not carried out on the acetone-d_6/SiO_2 sample because the ^{13}C CP-MAS signal intensity was too weak for this sample.

One can see that the $T_{1\rho}{}^H$ values of the methyl and carbonyl carbons are 29 and 30 ms, respectively, for acetone/SiO_2 and 28 and 32 ms, respectively, for acetone/SiO_2(d). The T_{CH} values of the methyl and carbonyl carbons are 11 and 17 ms, respectively, for acetone/SiO_2, 9 and 14 ms, respectively, for acetone/SiO_2(d), and 34 and 43 ms for acetone-d_6/SiO_2. One can also see that, for the acetone/SiO_2 and acetone/SiO_2(d) samples, the T_{CH} and $T_{1\rho}{}^H$ values of either methyl or carbonyl carbons are very similar between the two samples. This indicates that the major proton source in the $^1H-{}^{13}C$ cross-polarization in the acetone/SiO_2 and acetone/SiO_2(d) samples are the protons of methyl groups of adsorbed acetone. The T_{CH} values of the methyl or carbonyl carbons of acetone-d_6/SiO_2 are quite different from the T_{CH} values of the methyl or carbonyl carbons of acetone/SiO_2 and acetone/SiO_2(d). This indicates that the main proton source of $^1H-{}^{13}C$ cross-polarization in the acetone-d_6/SiO_2 system are the silanol protons of the silica surface (rather than the 5% of methyl hydrogens that are protons because of $^1H-{}^2H$ chemical exchange with surface silanols).

Variable-Temperature ^{13}C NMR Studies

Expected Behavior. According to the two-state adsorption model discussed above, there are two kinds of acetone species on the silica surface in terms of mobility, less mobile species (hydrogen-bonded acetone) and highly mobile physisorbed species (non-hydrogen-bonded acetone). In this model, at room temperature, hydrogen-bonded acetone molecules jump from one surface silanol site to another and/or rotate rapidly about the hydrogen-bonding axis and/or jump to a physisorption site. Because of fast chemical exchange between highly mobile and less mobile species at room temperature, it is impossible at that temperature to distinguish between the highly mobile and less mobile species directly via separate NMR signals. Because of the rapid dynamics of acetone molecules at room temperature, the observed chemical shifts and relaxation parameters are the time/motion averages of the corresponding parameter experienced in each state (hydrogen-bonded adsorption state and non-hydrogen-bonded adsorption state). To probe the dynamics, the sample temperature was decreased in order to slow chemical exchange, and perhaps molecular motion, of acetone on the silica surface. If the exchange of acetone from one state to another were slow enough and if there were two kinds of adsorbed species (hydrogen-bonded and non-hydrogen-bonded), major

differences between low-temperature ^{13}C DP-MAS and CP-MAS spectra of acetone/SiO_2 might be observed, or different chemical shifts (especially for the carbonyl carbon) might be observed for acetone species in the two different states.

Variable-Temperature ^{13}C DP-MAS Studies of Pure Acetone. Variable temperature (124−297 K) ^{13}C DP-MAS NMR spectra were obtained on pure natural-abundance acetone. Each spectrum was obtained with high-power ^1H decoupling and with a short ^{13}C pulse (3 μs, 54°), 500 repetitions, and a 3 s repetition delay. The line widths of the methyl and carbonyl peaks of pure acetone were each found to vary between 21 and 34 Hz over the temperature range. The corresponding variations of the carbonyl and methyl chemical shifts were 205.9−209.5 ppm and 30.6−30.9 ppm, respectively. Details are available elsewhere.[35]

The freezing point of pure acetone is 179 K. The line widths of the methyl and carbonyl peaks of pure acetone are the same and unchanged (20.6 Hz, 0.9 ppm) as the temperature is decreased from 297 to 188 K, i.e., above the freezing point. As the temperature is decreased from 188 to 124 K, the line widths of the methyl and carbonyl peaks of pure acetone are slightly broadened, i.e., about 28, 34, and 34 Hz at 166, 140, and 124 K, respectively, for both the methyl and carbonyl peaks. This indicates that the line width of pure, frozen, natural-abundance acetone would not vary much within the temperature range of this study (297−124 K).

There is no substantial chemical shift change of the methyl peak observed for pure acetone as the temperature is decreased[47−50] from 297 to 124 K. However, the chemical shift of the carbonyl peak of pure acetone moves about 3.6 ppm as the temperature is decreased from 188 to 124 K. It has been reported that the ^{17}O chemical shift of pure acetone moves to higher shielding and the ^{13}C chemical shift of the carbonyl peak of pure acetone moves to lower shielding as the temperature is decreased.[47−50] These shifts have been interpreted as due to a concentration increase of acetone dimers as the temperature is decreased, although the structure of the dimer is still open to debate, with both a *cyclic dimer* (with two "hydrogen bonds" between a methyl group of one acetone unit and the carbonyl oxygen of another unit)[51] and an *electrostatic collision complex* (two head-to-tail acetone units in two parallel planes at a distance of about 3.15 Å, with a C···O interaction between the carbonyl oxygen of one acetone molecule and the carbonyl carbon of another acetone molecule).[47−50,52,53]

Variable-Temperature ^{13}C CP-MAS and DP-MAS Studies of (Acetone-1-$^{13}C/SiO_2$ + Acetone-2-$^{13}C/SiO_2$). Variable-temperature (300−129 K) ^{13}C CP-MAS spectra were obtained on an acetone/SiO_2(θ = 0.80) sample prepared from roughly equal quantities of acetone-1-^{13}C (*CH_3COCH_3, 95% ^{13}C) and acetone-2-^{13}C (CH_3*$COCH_3$, 99% ^{13}C). Each spectrum (shown elsewhere)[35] was obtained with 400 repetitions, a 3 s repetition delay, and various CP contact times. The line widths and chemical shifts of the methyl and carbonyl peaks at each temperature are listed in Table 4. The CP contact time employed for each temperature (listed in Table 4) was decreased from 30 to 1 ms as the temperature was decreased from 300 to 129 K in order to obtain the maximum signal intensity.

The ratio of acetone-2-$^{13}C/SiO_2$ to acetone-1-$^{13}C/SiO_2$ is 1.2 in the (acetone-1-$^{13}C/SiO_2$ + acetone-2-$^{13}C/SiO_2$)(θ = 0.80) sample; this ratio was calculated from the integrated peak intensities of a DP-MAS spectrum, taking into account the ^{13}C spin−lattice relaxation factors. However, the intensity of the methyl peak is larger than that of the carbonyl peak in the CP-MAS spectra because the CP spin dynamics for the two carbons are different.

TABLE 4: ^{13}C CP-MAS and DP-MAS Results on Acetone-1-$^{13}C/SiO_2$ + Acetone-2-$^{13}C/SiO_2$(θ = 0.80) as a Function of Temperature (and CP Contact Time)

		line width (Hz)[c]				chemical shift (ppm)[d]			
		CP-MAS		DP-MAS		CP-MAS		DP-MAS	
T (K)[a]	t_{CP}[b] (ms)	C=O	CH_3	C=O	CH_3	C=O	CH_3	C=O	CH_3
300	30	21	21	21	21	214.7	30.0	215.0	30.0
263	30	21	21	21	21	215.0	30.0	215.2	30.0
237	20	28	28	28	28	215.3	29.7	215.5	29.7
210	7	69	41	55	34.4	215.8	29.7	215.9	29.7
183	5	151	55	178	41	216.4	29.7	216.4	29.7
172	1	247	55	234	55	216.8	29.7	216.8	29.7
157	1	247	69	234	55	217.4	29.7	217.2	29.7
142	1	247	69	220	55	217.8	29.7	217.7	29.7
129	1	220	69	220	55	217.7	29.4	217.7	29.5

[a] Estimated error, ±2 K. [b] CP contact time in CP-MAS experiments. [c] Estimated error, ±5%. [d] Estimated error, ±0.3 ppm.

The isotropic chemical shifts of the methyl and carbonyl peaks of (acetone-1-$^{13}C/SiO_2$ + acetone-2-$^{13}C/SiO_2$)(θ = 0.80) move as the temperature is decreased from 300 to 129 K (Table 4), from 214.7 to 217.7 ppm for the carbonyl peak and from 30.0 to 29.4 ppm for the methyl peak. The parameter $\Delta\delta$ (= $\delta_{C=O} - \delta_{CH_3}$ ppm) gradually increases from 184.7 to 188.3 ppm as the temperature is decreased from 300 to 129 K.

As the sample temperature is decreased from 300 to 129 K, the chemical shift difference, $\Delta\delta$, of the (acetone-1-$^{13}C/SiO_2$ + acetone-2-$^{13}C/SiO_2$)(θ = 0.80) sample increases from 8.6 to 12.2 ppm, presumably because of the increase in the fraction of acetone that is hydrogen bonded. When the fraction of acetone that is hydrogen-bonded is larger, the observed chemical shifts will be closer to the chemical shifts of hydrogen-bonded acetone and the chemical shift difference will be larger. The fact that the fraction of acetone that is hydrogen bonded increases as the temperature is decreased is what one expects if the equilibrium constant (K) between physisorbed acetone molecules on the surface, potential hydrogen-bonding surface sites that are not occupied by acetone, and hydrogen-bonded complexes on the surface (eq 2) increases as the temperature is decreased. This behavior can be understood in terms of the Helmholtz equation,

$$\ln K = \frac{-\Delta H^\circ}{RT} + \frac{\Delta S^\circ}{R} \tag{11}$$

where ΔH° and ΔS° are the enthalpy and entropy changes for the reaction shown in eq 2. For the present purposes, we define the standard state for each species represented in eq 2 as a state with one such structural unit (su) per nm^2 on the surface.

If the enthalpy and entropy terms are independent of the temperature, then the second factor on the right side of eq 11 is independent of the temperature, and the temperature dependence of the equilibrium constant results only from the dependence of the first factor on the right side of the equation

$$\left[\frac{\partial \ln K}{\partial (1/T)}\right]_P = -\frac{\Delta H^\circ}{R} \tag{12}$$

If, as expected in the present case, the formation of hydrogen-bonded acetone is an exothermic reaction, then the equilibrium constant increases as the temperature is decreased, a prediction that is consistent with the fact that the chemical shift difference increases as the temperature is decreased.

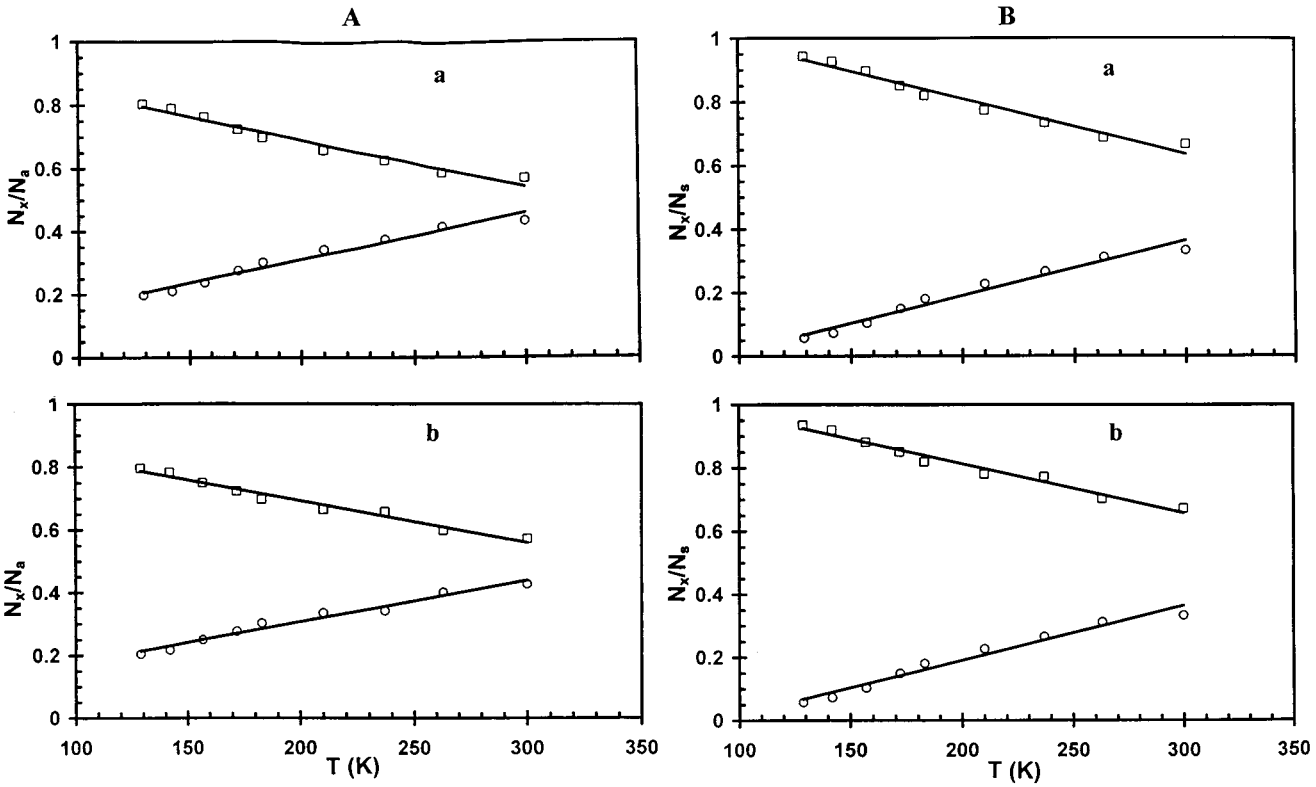

Figure 6. (A) (left). Plots of the fraction of hydrogen-bonded acetone (N_{hb}/N_a) and the fraction of non-hydrogen-bonded acetone ($1 - N_{hb}/N_a$) of (acetone-1-^{13}C/SiO_2 + acetone-2-^{13}C/SiO_2)($\theta = 0.80$) as functions of sample temperature: points ((□) for N_{hb}/N_a and (○) for $1 - N_{hb}/N_a$), obtained from (a) ^{13}C CP-MAS and (b) ^{13}C DP-MAS chemical shift measurements according to eq 4. Each line is a computer least-squares linear fit of the points. (B) (right). Plots of the fraction of hydrogen-bonding surface sites (silanols) that are occupied (N_{hb}/N_s) and the fraction of hydrogen-bonding surface sites that are unoccupied ($1 - N_{hb}/N_s$) of (acetone-1-^{13}C/SiO_2 + acetone-2-^{13}C/SiO_2)($\theta = 0.80$) as functions of sample temperature: points ((□) for N_{hb}/N_s and (○) for $1 - N_{hb}/N_s$). N_{hb} values were obtained according to eq 4 and $N_s = 1.5$ acetone/nm^2. Each line is a computer least-squares linear fit of the points: (a) ^{13}C CP-MAS and (b) ^{13}C DP-MAS.

Equation 4 was used to calculate the number of hydrogen-bonded acetone molecules (N_{hb}) per nm^2 in an acetone/SiO_2 system from the observed chemical shift at each temperature, and eq 3 was then used to calculate the equilibrium constant at each temperature.

Parts A-a and A-b of Figure 6 show plots of the temperature dependence of the fractions of hydrogen-bonded and non-hydrogen-bonded acetone on the (acetone-1-^{13}C/SiO_2 + acetone-2-^{13}C/SiO_2)($\theta = 0.80$) surface (N_{hb}/N_a and $1 - N_{hb}/N_a$) obtained according to eq 4 as functions of the temperature for ^{13}C MAS experiments. One can see that the fraction of hydrogen-bonded acetone increases from about 57% to 80% as the temperature is decreased from 300 to 129 K.

Parts B-a and B-b of Figure 6 show plots of the temperature dependence of the fractions of hydrogen-bonded surface sites (silanols) that are occupied and that are unoccupied on the (acetone-1-^{13}C/SiO_2 + acetone-2-^{13}C/SiO_2)($\theta = 0.80$) surface (N_{hb}/N_s and $1 - N_{hb}/N_s$) as functions of the temperature for ^{13}C MAS experiments. The N_{hb} values were derived from eq 4 and $N_s = 1.5$ acetone/nm^2. The fractions of hydrogen-bonded and non-hydrogen-bonded acetone on the (acetone-1-^{13}C/SiO_2 + acetone-2-^{13}C/SiO_2)($\theta = 0.80$) surface (N_{hb}/N_a and $1 - N_{hb}/N_a$), the fractions of hydrogen-bonding surface sites (silanols) that are occupied and that are unoccupied on the (acetone-1-^{13}C/SiO_2 + acetone-2-^{13}C/SiO_2)($\theta = 0.80$) surface (N_{hb}/N_s and $1 - N_{hb}/N_s$), and the equilibrium constant (K) for the formation of hydrogen-bonded complexes at each temperature for the ^{13}C MAS experiments are listed in Table 5.

Figure 7 shows a plot of the experimental ln K values vs $1/T$ for the (acetone-1-^{13}C/SiO_2 + acetone-2-^{13}C/SiO_2)($\theta = 0.80$) system for the temperature range from 300 to 129 K; also shown are the computer-based least-squares fit of the data for ^{13}C MAS experiments. The $\Delta H°$ and $\Delta S°$ values derived from this fit for acetone adsorbed on the silica surface are -5.8 ± 0.3 kJ mol^{-1} and -12.5 ± 0.7 J K^{-1}mol^{-1}, respectively. The negative $\Delta H°$

TABLE 5: ^{13}C CP-MAS Results Derived from Eqs 3, 4, and 11 on Acetone-1-^{13}C/SiO_2 + Acetone-2-^{13}C/SiO_2($\theta = 0.80$) as a Function of Temperature

T (K)[a]	N_a[b]	N_{hb}/N_a[c]	N_{hb}[d]	$1 - N_{hb}/N_a$[e]	N_{nh}[f]	N_s[g]	$N_s - N_{hb}$[h]	K[i] (nm^2/su)
300	1.76	0.57	1.00	0.43	0.76	1.50	0.50	2.6
263	1.76	0.59	1.03	0.41	0.73	1.50	0.47	3.0
237	1.76	0.63	1.10	0.37	0.66	1.50	0.40	4.2
210	1.76	0.66	1.16	0.34	0.60	1.50	0.34	5.7
183	1.76	0.70	1.23	0.30	0.53	1.50	0.27	8.6
172	1.76	0.73	1.28	0.27	0.48	1.50	0.22	12
157	1.76	0.76	1.34	0.24	0.42	1.50	0.16	20
142	1.76	0.79	1.39	0.21	0.37	1.50	0.11	34
129	1.76	0.80	1.41	0.20	0.35	1.50	0.09	45

[a] Estimate error, ±2 K. [b] N_a is the total number of acetone molecules (per nm^2) present on the silica surface. Estimated error, ±6%. [c] N_{hb}/N_a were obtained from chemical shift measurements according to eq 4. Estimated error, ±7%. [d] N_{hb} is the number of hydrogen-bonded acetone (per nm^2) on the silica surface and was obtained according to eq 4. Estimated error, ±6%. [e] $(1 - N_{hb}/N_a)$ were obtained from chemical shift measurements according to eq 4. Estimated error, ±7%. [f] N_{nh} is the number of non-hydrogen-bonded acetone (per nm^2) on the silica surface. Estimated error, ±6%. [g] N_s is the total number of silanol adsorption sites (per nm^2) on the surface. Estimated error, ±6%. [h] $(N_s - N_{hb})$ is the number of hydrogen bonding sites (silanols) that are unoccupied. Estimated error, ±6%. [i] K is the equilibrium constant for the formation of hydrogen-bonded complexes. Estimated error, ±10%.

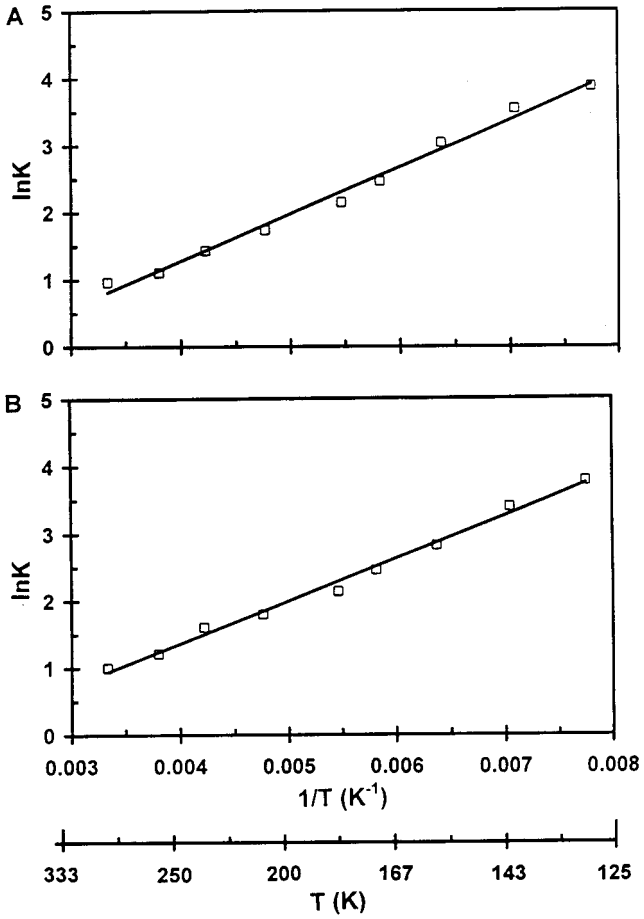

Figure 7. Plot of the experimental ln *K* (points, derived from eq 3) as a function of temperature for (A) ^{13}C CP-MAS and (B) ^{13}C DP-MAS, and the fitting line (eq 11) for (acetone-1-^{13}C/SiO_2 + acetone-2-^{13}C/SiO_2)($\theta = 0.80$).

value indicates that the formation of ⟨Si⟩OH···O=C$(CH_3)_2$ complexes from physisorbed acetone is an exothermic reaction. These parameters correspond to $\Delta H_{(1)}°$ and $\Delta S_{(1)}°$ in Figure 8.

Reported values of $\Delta H°$ for the formation of hydrogen-bonded complexes of acetone with liquid alcohols, acetic acid, water, and chloroform range from about −3.3 to −46 kJ mol^{-1}.[54−56] These $\Delta H°$ values correspond to $\Delta H_{(2)}°$ in Figure 8 and relate to the following equilibrium:

$$CH_3COCH_3\,(liq) + XH\,(liq) \underset{\Delta H_{(2)}°}{\rightleftharpoons} XH\cdots O{=}C(CH_3)_2\,(liq)$$

where XH stands for acetic acid, water, or chloroform. Values reported for the heat of adsorption (ΔH) of acetone on silica from the gas phase range from 30 to 75 kJ mol^{-1}.[11,57,58] These $\Delta H°$ values correspond to some linear combination of ΔH_{ad} and $\Delta H_{(3)}°$ in Figure 8, where ΔH_{ad} refers here to physisorption from the gas phase and $\Delta H_{(3)}°$ corresponds to the process

$$CH_3COCH_3\,(gas) + \langle Si\rangle OH \underset{\Delta H_{(3)}°}{\rightleftharpoons} \langle Si\rangle OH\cdots O{=}C(CH_3)_2 \qquad (13)$$

The weighting factors in this linear combination depend on the concentration and distribution of silanols on the silica surface and on the acetone loading level.

In general, physisorption has a comparatively small enthalpy of adsorption, typically in the range −4 to −40 kJ mol^{-1}, while a wide range of enthalpy changes may occur on chemisorption, with typical values ranging from −65 to −90 kJ mol^{-1}.[59−61] The $\Delta H_{(1)}°$ value derived in our study for the transformation of non-hydrogen-bonded acetone on the silica surface is about −5.8 kJ mol^{-1}, which is within the range of previously reported $\Delta H_{(2)}°$ values (−3.3 to −46 kJ mol^{-1}) for the formation of hydrogen-bonded complexes of acetone with protonic solvents in the liquid state.[54−56] Then, if we assume that the molar enthalpy of *physisorbed* acetone is similar to the molar enthalpy of liquid-state acetone and recognize that the enthalpy of vaporization of acetone from the liquid state to the gaseous state is 31.2 kJ mol^{-1},[62] we can estimate $\Delta H_{(3)}°$ as follows: $\Delta H_{(3)}° = \Delta H_{(1)}° - \Delta H°_{liq/phys} - \Delta H_{vap} \approx -5.8 + 0 - 31.2 = -37$ kJ mol^{-1}, which is within the range of previously reported ΔH values (−30 to −75 kJ mol^{-1}) for the formation of hydrogen-bonded complexes of acetone with silanol groups of the silica surface from the gas phase.[56−58]

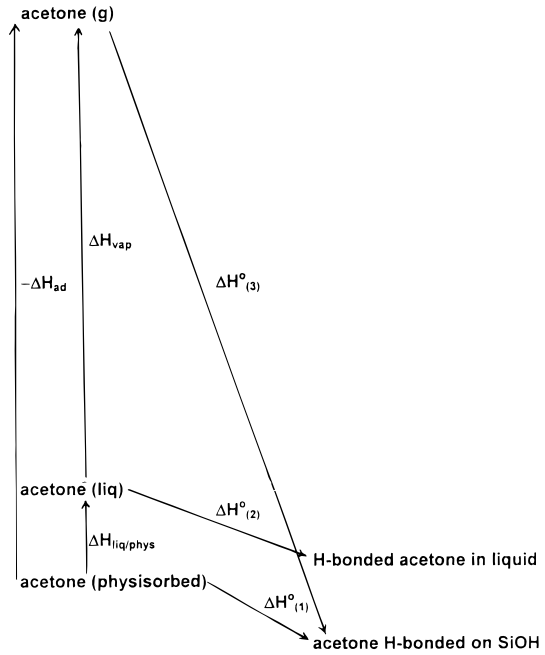

Figure 8. "Cartoon" diagram of various states of non-hydrogen-bonded acetone (on the left) and hydrogen-bonded acetone (on the right).

Conclusions

A large body of ^{13}C-derived and ^{29}Si-derived chemical shift and relaxation data can be interpreted in terms of a two-state model in which acetone molecules are in a rapid equilibrium between a non-hydrogen-bonded state in which acetone is physisorbed to the silica surface and a state in which acetone molecules are hydrogen bonded to silanol (SiOH) groups of the silica surface. The relaxation parameters can be rationalized in terms of the relative mobilities of these states. Analysis of the peak position data in terms of acetone loading level and temperature yields values of *K*, $\Delta H°$, and $\Delta S°$ that are compatible with previously reported results.

Acknowledgment. The authors gratefully acknowledge the assistance of Dr. Jincheng Xiong and partial financial support from the U.S. Department of Energy by Grant DE-FG03-95ER14558.

Supporting Information Available: Much of the NMR data is available, including the $\theta = 0.20$ analogue of Figure 1 and 10 "relaxation curves" corresponding to the time-domain experiments carried out to measure T_1^C, T_1^H, $T_{1\rho}^H$, and T_{CH} on the samples of this study. Also available is a table of data on the ^{13}C NMR prameters of pure acetone from 124 to 297 K.

This material is available free of charge via the Internet at http://pubs.acs.org.

References and Notes

(1) Bergna, H. E. The Colloid Chemistry of Silica. *ACS Adv. Chem. Ser.* **1994**, *234*, 1.
(2) Iler, R. K. *The Chemistry of Silica*; Wiley: New York, 1979.
(3) *Porous Silica*; Unger, K. K., Ed.; Elsevier Publishing Company: New York, 1979.
(4) Van Der Voort, P.; Vansant, E. F. *J. Liq. Chromatogr. Relat. Technol.* **1996**, *19*, 2723.
(5) Plueddemann, E. P. *J. Adhesion Sci. Technol.* **1991**, *5*, 261.
(6) Goodwin, J. W.; Harbron, R S.; Reynolds, P. A. *Colloid Polym. Sci.* **1990**, *268*, 766.
(7) Maciel, G. E.; Ruben, G. C. *J. Am. Chem. Soc.* **1963**, *42*, 3903.
(8) Maciel, G. E.; Natterstad, J. J. *J. Chem. Phys.* **1965**, *42*, 2752.
(9) Young, R. P.; Sheppard, N. *J. Catal.* **1967**, *7*, 223.
(10) Young, R. P.; Sheppard, N. *Trans. Faraday Soc.* **1967**, *63*, 2291.
(11) Hertl, W.; Hair, M. L. *J. Phys. Chem.* **1968**, *72*, 4676.
(12) Hair, M. L.; Hertl, W. *J. Phys. Chem.* **1968**, *72*, 4269.
(13) Elkington, P. A.; Curthoys, G. *J. Phys. Chem.* **1968**, *72*, 3475.
(14) Mioc, U. B.; Bogunovic, Lj. J.; Ribnikar, S. V.; Dragojevic, M. D. *J. Mol. Struct.* **1988**, *177*, 379.
(15) McManus, J. C.; Harano, Y.; Low, M. J. D. *Can. J. Chem.* **1969**, *47*, 2545.
(16) Hair, M. L.; Hertl, W. *J. Phys. Chem.* **1970**, *74*, 91.
(17) Thomas, G.; Eon, C. H. *J. Colloid Interface Sci.* **1977**, *62*, 259.
(18) Nasuto, R. *Roczniki Chem.* **1977**, *51*, 515.
(19) Nasuto, R. *Roczniki Chem.* **1977**, *51*, 525.
(20) Gavrilov, K.; Kutsovskiy, Y.; Paukshtis, E.; Okunev, A.; Aristov, Y. *Mol. Cryst. Liq. Cryst.* **1994**, *248*, 159.
(21) Airoldi, C.; Santos, L. S., Jr. *Thermochim. Acta* **1986**, *104*, 111.
(22) Gay, I. D. *J. Phys. Chem.* **1974**, *78*, 38.
(23) Slofeldt-Ellingsen, D.; Bibow, B.; Pederson, B. In *Magnetic Resonance in Colloid and Interface Science*; Fraissard, J. P., Resing, H. A., Eds.; Reidel Publishing Co.: Dordrecht 1980; p 571.
(24) Borovkov, V. Y.; Zaiko, A. V.; Kazansky, V. B.; Hall, W. K. *J. Catal.* **1982**, *75*, 219.
(25) Bernstein, T.; Michel, D.; Pfeifer, H.; Fink, P. *J. Colloid Interface Sci.* **1981**, *84*, 310.
(26) Fyfe, C. A. *Solid-State NMR for Chemists*; C. F. Press: Guelph, 1983; p 268.
(27) Andrew, E. R. *Prog. NMR Spectrosc.* **1971**, *8*, 1.
(28) Pines, A.; Gibby, W. G.; Waugh, J. S. *J. Chem. Phys.* **1973**, *59*, 509.
(29) Schaefer, J.; Stejskal, E. O. *J. Am. Chem. Soc.* **1976**, *98*, 1031.
(30) Furniss, B. S.; Hannaford, A. J.; Smith, P. W. G.; Tatchell, A. R. *Vogel's Textbook of Practical Organic Chemistry*; Wiley: New York, 1989; p 604.
(31) Frye, J. *Concepts Magn. Reson.* **1989**, *1*, 27.
(32) Mehring, M. *Principles of High-Resolution NMR in Solids*, 2nd ed.; Springer-Verlag: New York, 1983; p 151.
(33) Schaefer, J.; Stejskal, E. O.; Buchdahl, R. *Macromolecules* **1977**, *10*, 384.
(34) Haw, J. F.; Speed, J. A. *J. Magn. Reson.* **1977**, *78*, 344.
(35) Available in the Supporting Information and in the following: Pan, V. H. ^{13}C and ^{29}Si NMR Investigation of Acetone Adsorbed on Silica Surfaces. Ph.D. Dissertation, Colorado State University, 1996.
(36) Demco, D. E.; Tegenfeldt, J.; Waugh, J. S. *Phys. Rev.* **1975**, *11*, 4133.
(37) Maciel, G. E.; Sindorf, D W. *J. Am. Chem. Soc.* **1980**, *102*, 7606.
(38) Chuang, I.-S.; Kinney, D. R.; Bronnimann, C. E.; Zeigler, R. C.; Maciel, G. E. *J. Am. Chem. Soc.* **1992**, *96*, 4027.
(39) Lyerla, J. R., Jr.; Levy, G. C. In *Topics Carbon-13 NMR Spectroscopy*; Levy, G. C., Ed.; 1974; p 79.
(40) Redfield, A. G. *IBM J.* **1957**, *1*, 19.
(41) Schaefer, J. In *Topics Carbon-13 NMR Spectroscopy*; Levy, G. C., Ed.; 1974; p 149.
(42) Schaefer, J. *Macromolecules* **1973**, *6*, 882.
(43) Douglass, D. C.; Jones, G. P. *J. Phys. Chem.* **1966**, *45*, 956.
(44) VanderHart, D. L.; Garroway, A. N. *J. Phys. Chem.* **1979**, *71*, 2773.
(45) Zeigler, R. C.; Maciel, G. E. *J. Phys. Chem.* **1991**, *95*, 7347.
(46) Maciel, G. E.; Sindorf, D. W. *J. Am. Chem. Soc.*, **1980**, *102*, 7606.
(47) Ancian, B.; Tiffon, B. A.; Dubios, J. E. *Chem. Phys.* **1983**, *74*, 171.
(48) Tiffon, B.; Ancian, B. *Org. Magn. Reson.* **1979**, *12*, 24.
(49) Tiffon, B.; Ancian, B. *Org. Magn. Reson.* **1981**, *16*, 247.
(50) Tiffon, B. A.; Dubios, J. E. *Chem. Phys. Lett.* **1980**, *73*, 89.
(51) Frurip, D. J.; Curtiss, L. A.; Blander, M. *J. Phys. Chem.* **1978**, *82*, 2555.
(52) Lumbroso-Bader, N.; Chenon, M. T.; Bouquant, J. *J. Chim. Phys.* **1970**, *67*, 1829.
(53) Lin, T. F.; Christian, B.; Affsprung, H. F. *J. Phys. Chem.* **1967**, *71*, 968.
(54) Balasubramanian, A.; Rao, C. N. R. *Spectrochim. Acta* **1962**, *18*, 1337.
(55) Becker, E. D. *Spectrochim. Acta* **1961**, *17*, 436.
(56) Matsui, T.; Hepler, L. G.; Fenby, D. V. *J. Phys. Chem.* **1973**, *77*, 2397.
(57) Curthoys, G.; Davydov, V. Y.; Kiselev, A. V.; Kiselev. S. A.; Kuznetsov, B. V. *J. Colloid Interface Sci.* **1974**, *48*, 58.
(58) Afsal, M.; Khan, M.; Ahmad, H. *J. Chem. Soc. Pak.* **1991**, *13*, 157.
(59) Gasser, R. P. H. *An Introduction to Chemisorption and Catalysis by Metals*; Clarendon Press: Oxford, 1985; p 1.
(60) Samorjai, G. A. *Chemistry in Two-Dimensional Surfaces*; Cornell University Press: Ithaca, New York, 1981; p 178.
(61) Tamaru, K. *Dynamic Heterogeneous Catalysis*; Academic Press: San Francisco, 1978; p 34.
(62) *CRC Handbook of Chemistry and Physics*, 79th ed.; Lide, D. R., Ed.; CRC Press: Boca Raton, 1989−1990; Section 6, p 105.